Analytic formula for estimating the α-particle preformation factor

Jun-Gang Deng (邓军刚) [1] and Hong-Fei Zhang (张鸿飞) [1,2,3,*]

[1] School of Nuclear Science and Technology, Lanzhou University, 730000 Lanzhou, People's Republic of China

[2] Joint Department for Nuclear Physics, Institute of Modern Physics, CAS and Lanzhou University, 730000 Lanzhou, People's Republic of China

[3] Engineering Research Center for Neutron Application, Ministry of Education, Lanzhou University, 730000 Lanzhou, People's Republic of China

(Received 2 June 2020; accepted 28 August 2020; published 14 October 2020)

In the present work, we build a bridge between the α decay energy and the α-particle preformation factor, and put forward an analytic formula for estimating the α-particle preformation factor. With the help of this formula, experimental α decay half-lives of 535 nuclei varying from 6.90×10^{-8} to 6.34×10^{26} s are reproduced within a factor of 1.81. Noticeably, for superheavy nuclei, calculated α decay half-lives can well reproduce experimental data and reduce the deviations significantly. This formula can be applied to estimate the α-particle preformation factors and predict the α decay half-lives for unsynthesized superheavy nuclei, which would be useful for future experiments in synthesizing new superheavy elements and isotopes. This formula can shed light on microscopic nuclear structure information such as shell and odd-even staggering effects, and provide a positive signal for the existence of an island of stability for superheavy nuclei.

DOI: 10.1103/PhysRevC.102.044314

I. INTRODUCTION

In 1928, Gurney and Condon [1] and Gamow [2] proposed the quantum tunneling theory to describe α decay. Quantum mechanics was used in nuclear physics for the first time, and not only explained the α decay process successfully but also promoted its development. In recent years, radioactive ion beam facilities and experiments worldwide focus on new nuclei far from the β-stability line. α decay is an important probe for studying unstable nuclei and neutron-deficient nuclei, and it is an important decay mode of heavy and superheavy nuclei that attracts a lot of interest [3–7]. From the researches on α decay, much important information on nuclear structure has been observed, such as the properties of the ground state, nuclear deformation, nuclear shape coexistence, energy levels, and so on [8–19]. In addition, observation of α decay is an important way to identify new synthesized superheavy nuclei [20–25]. Besides, it is meaningful to unify proton radioactivity, α decay, cluster radioactivity, and spontaneous fission in one physical picture of barrier penetration [26–38]. Therefore, α decay is one of the hottest topics in the field of nuclear physics.

Within Gamow's theory, the α decay process is described as a preformed α particle penetrating the Coulomb barrier. Hence an α-particle preformation factor hypothesis is proposed to describe the probability of an α-cluster formation inside its parent nucleus before emission. The α-particle preformation factor depends heavily on the state structures of parent and daughter nuclei, and is a measure of the similarity between the initial state of the parent nucleus and the final state of the daughter nucleus plus α particle [39]. There are many models devoted to estimating the α-particle preformation factor. Microscopically, the α-particle preformation factor can be obtained by the overlap between the initial wave function and the α decaying wave function [40]. In the R-matrix method, the α-particle preformation factor is calculated by the initial tailored wave function of the parent nucleus [41–44]. The Tohsaki-Horiuchi-Schuck-Röpke wave function approach can successfully describe the cluster structure of light nuclei and the α-particle preformation factor [45,46]. Because of the complicated structure of quantum many-body systems, microscopic methods are extremely difficult for calculation the α-particle preformation factor of a nucleus that is heavier than ^{212}Po.

Phenomenologically, the α-particle preformation factor, P_α, is obtained from the ratio of the theoretical α decay half-life to the experimental value; in the theoretical calculation, P_α is a constant [39,47–51]. However, the extrapolations of the α-particle preformation factor and half-life for an unknown nucleus by this method are limited to some extent. Recently, the cluster-formation model (CFM) was proposed to extract the α-particle preformation factor using binding energy differences of the parent nucleus and its neighboring nuclei [28,52–55]. But, at present, CFM cannot be generalized to the isomeric state. Therefore, there is an urgent need to establish a new method for accurately describing the α-particle preformation factor globally. This is the purpose of the present work.

The Royer formula [56–58] and the universal decay law (UDL) [59] have achieved great successes in describing α decay half-lives [60–69]. In the present work, we build a

*zhanghongfei@lzu.edu.cn

bridge between the α decay energy and α-particle preformation factor with the help of an empirical formula for α decay half-lives, and put forward an analytical expression for estimating the α-particle preformation factor. This formula can be used to accurately calculate α decay half-lives, and can be extended to estimate α-particle preformation factors as well as predict α decay half-lives for unsynthesized superheavy nuclei. This formula can also shed light on some microscopic nuclear structure information such as the shell effect and the odd-even staggering effect. This article is organized as follows. In Sec. II, the theoretical framework of the α decay half-life is briefly presented. The analytic formula for estimating α-particle preformation factor is put forward. The detailed calculations and discussion are given in Sec. III. Section IV is a brief summary.

II. THEORETICAL FRAMEWORK

A. The generalized liquid drop model

The α decay half-life can be obtained by

$$T_{1/2} = \frac{\ln 2}{\lambda}. \tag{1}$$

In the framework of the generalized liquid drop model (GLDM) [39,64,70–73], the α decay constant λ is calculated by

$$\lambda = P_\alpha \nu P, \tag{2}$$

where P_α represents the α-particle preformation factor. The assault frequency ν is expressed as

$$\nu = \frac{1}{2R_0}\sqrt{\frac{2E_\alpha}{M_\alpha}}, \tag{3}$$

where R_0 denotes the radius of the α decay parent nucleus, which can be obtained by

$$R_i = 1.28A_i^{1/3} - 0.76 + 0.8A_i^{-1/3} \quad (i = 0, 1, 2). \tag{4}$$

$E_\alpha = \frac{A-4}{A} Q_\alpha$ is the kinetic energy of the α particle, with A and Q_α being the mass number and α decay energy of the parent nucleus. M_α represents the mass of the α particle.

Using the Wentzel-Kramers-Brillouin (WKB) approximation, the barrier penetrating probability P is expressed as

$$P = \exp\left[-\frac{2}{\hbar}\int_{r_{\rm in}}^{r_{\rm out}} \sqrt{2B(r)[E_r - E(\text{sphere})]}dr\right], \tag{5}$$

where r is the center-of-mass distance between the α cluster and daughter nucleus. The classical turning points $r_{\rm in}$ and $r_{\rm out}$ satisfy the conditions $r_{\rm in} = R_1 + R_2$ and $E(r_{\rm out}) = Q_\alpha$. $B(r) = \mu$ denotes the reduced mass between the α particle and daughter nucleus.

The total interaction potential E in GLDM includes four parts [56]: the volume energy E_V, the surface energy E_S, the Coulomb energy E_C, and the proximity energy $E_{\rm Prox}$. In this work, the centrifugal potential E_l is introduced into the GLDM to study the unfavored α decay:

$$E = E_V + E_S + E_C + E_{\rm Prox} + E_l. \tag{6}$$

For one-body shapes, the volume, surface, and Coulomb energies are defined as

$$E_V = -15.494(1 - 1.8I^2)A, \tag{7}$$

$$E_S = 17.9439(1 - 2.6I^2)A^{2/3}\left(S/4\pi R_0^2\right), \tag{8}$$

$$E_C = 0.6e^2(Z^2/R_0) \times 0.5\int [V(\theta)/V_0](R(\theta)/R_0]^3 \sin\theta\, d\theta, \tag{9}$$

where S denotes the surface of the one-body deformed nucleus. I is the relative neutron excess. $V(\theta)$ represents the electrostatic potential at the surface and V_0 the surface potential of the sphere.

When the fragments are separated,

$$E_V = -15.494\left[\left(1 - 1.8I_1^2\right)A_1 + \left(1 - 1.8I_2^2\right)A_2\right], \tag{10}$$

$$E_S = 17.9439\left[\left(1 - 2.6I_1^2\right)A_1^{2/3} + \left(1 - 2.6I_2^2\right)A_2^{2/3}\right], \tag{11}$$

$$E_C = 0.6e^2Z_1^2/R_1 + 0.6e^2Z_2^2/R_2 + e^2Z_1Z_2/r, \tag{12}$$

where A_i, Z_i, R_i, and I_i denote the mass numbers, proton numbers, radii, and the relative neutron excesses of the α particle and daughter nucleus, respectively. The radii R_i can be calculated by Eq. (4).

GLDM can describe the complex deformation process from parent nucleus continuous transition to the appearance of deep and narrow necks, and finally into two tangential fragments, because it introduces the quasimolecular shape mechanism [56]. All along the decay path, the effects of the nucleon-nucleon force inside the neck or the gap between the nascent or separated α particle and daughter nucleus have been taken into account in a proximity energy term [56], which can be expressed as

$$E_{\rm Prox}(r) = 2\gamma \int_{h_{\rm min}}^{h_{\rm max}} \Phi[D(r,h)/b]2\pi h\, dh, \tag{13}$$

with the surface parameter γ being the geometric mean between the surface parameters of the two fragments:

$$\gamma = 0.9517\sqrt{\left(1 - 2.6I_1^2\right)\left(1 - 2.6I_2^2\right)}, \tag{14}$$

where h is the ring radius in the plane perpendicular to the longitudinal deformation axis. D denotes the distance between the opposite infinitesimal surfaces [74]. After the separation, $h_{\rm min} = 0$ and $h_{\rm max} = R_1$. $b = 0.99$ fm is the standard surface width value [56]. Φ denotes the proximity function.

The centrifugal barrier $E_l(r)$ is expressed as

$$E_l(r) = \frac{\hbar^2 l(l+1)}{2\mu r^2}, \tag{15}$$

where l is the angular momentum carried by the α particle. Based on the conservation of angular momentum and parity [60], the minimum angular momentum $l_{\rm min}$ taken away by the α particle is expressed as

$$l_{\rm min} = \begin{cases} \Delta_j & \text{for even } \Delta_j \text{ and } \pi_p = \pi_d, \\ \Delta_j + 1 & \text{for even } \Delta_j \text{ and } \pi_p \neq \pi_d, \\ \Delta_j & \text{for odd } \Delta_j \text{ and } \pi_p \neq \pi_d, \\ \Delta_j + 1 & \text{for odd } \Delta_j \text{ and } \pi_p = \pi_d, \end{cases} \tag{16}$$

TABLE I. The parameters of Eq. (21), and standard deviations between estimated α-particle preformation factors by Eq. (21) and extracted experimental α-particle preformation factors from Eq. (20).

Nuclei	Region	a	b	c	d	e	f	σ
Even-even nuclei	$N \leqslant 126$	−9.8980	−8.5241	4.3520	1.1231	−2.8566		0.213
	$N > 126$	−2.9300	−0.0571	4.4151	1.1214	−0.0123		
Odd-A nuclei	$N \leqslant 126$	−27.1693	−13.5635	11.2042	2.8926	−4.7185	−0.0338	0.285
	$N > 126$	1.3776	−6.0618	−0.2476	−0.0733	−1.8972	−0.0913	
Doubly odd nuclei	$N \leqslant 126$	−1.5349	−4.1063	1.5502	0.4059	−1.3209	−0.0912	0.231
	$N > 126$	−38.3925	−20.2893	23.7471	6.1166	−7.0236	−0.2007	

where $\Delta_j = |j_p - j_d|$. j_p, π_p, j_d, π_d are the spin and parity values of the parent and daughter nuclei, respectively.

B. The α-particle preformation factor

The experimental α decay constant $\lambda_{\rm exp}$ can be obtained by experimental α decay half-life $T_{1/2}^{\rm exp}$,

$$\lambda_{\rm exp} = \frac{\ln 2}{T_{1/2}^{\rm exp}} = P_\alpha \nu P. \tag{17}$$

If the α-particle preformation factor fixed as a constant, $P_0 = 1$, the theoretical decay constant $\lambda_{\rm cal}$ is

$$\lambda_{\rm cal} = \frac{\ln 2}{T_{1/2}^{\rm cal}} = P_0 \nu P. \tag{18}$$

Thus experimental α-particle preformation factor P_α can be extracted from experimental α decay half-life [39,47–51] because the α decay half-life is mainly decided by the barrier penetrating probability [39]. It is expressed as

$$P_\alpha^{\rm exp} = \frac{\lambda_{\rm exp}}{\lambda_{\rm cal}} = \frac{T_{1/2}^{\rm cal}}{T_{1/2}^{\rm exp}}. \tag{19}$$

Taking the logarithms of both sides of Eq. (19), we have

$$\log_{10} P_\alpha^{\rm exp} = \log_{10} \frac{T_{1/2}^{\rm cal}}{T_{1/2}^{\rm exp}} = \log_{10} T_{1/2}^{\rm cal} - \log_{10} T_{1/2}^{\rm exp}. \tag{20}$$

Two empirical formulas for α decay half-life, namely the Royer formula [56–58] and the UDL formula [59], which both successfully describe the α decay [60–69], are used here to express $\log_{10} T_{1/2}^{\rm cal}$ and $\log_{10} T_{1/2}^{\rm exp}$, respectively. Then, we put forward an analytic expression for estimating the α-particle preformation factor:

$$\log_{10} P_\alpha^{\rm Eq} = a + bA^{1/6}\sqrt{Z} + c\frac{Z}{\sqrt{Q_\alpha}} - d\chi' - e\rho' + f\sqrt{l(l+1)}, \tag{21}$$

where the first three terms come from the Royer formula [56–58]. The fourth term $\chi' = Z_1 Z_2 \sqrt{\frac{A_1A_2}{(A_1+A_2)Q_\alpha}}$ and fifth term $\rho' = \sqrt{\frac{A_1A_2}{A_1+A_2} Z_1 Z_2 (A_1^{1/3} + A_2^{1/3})}$ are from the UDL formula [59]. The last term depends on the angular momentum carried by the α-particle and reflects the hindrance effect of the centrifugal potential. It is notable that this term is independent of mass. With the help of Eq. (20) and calculated α decay half-lives with $P_0 = 1$ in GLDM as well as corresponding experimental data, the values of adjustable parameters a, b, c, d, e, and f are listed in Table I. Equation (21) builds a bridge between the α decay energy and α-particle preformation factor. If α decay energy is obtained, ones can easily estimate the α-particle preformation factor. Therefore, Eq. (21) is helpful to calculate and predict α decay half-life exactly as well as shed light on some microscopic nuclear structure information.

III. RESULTS AND DISCUSSION

The GLDM can well deal with the proton radioactivity [32], cluster radioactivity [75], fusion [74], fission [76], and the α decay process [39,56,64,70–73]. Here, first, we adopt the GLDM to calculate α decay half-lives with $P_\alpha = 1$ for 159 even-even nuclei, 295 odd-A nuclei, and 81 doubly odd nuclei. The calculations are denoted as $\log_{10} T_{1/2}^{\rm cal1}$ and listed in Tables II–IV. Then we use Eq. (20) with calculated α decay half-lives $\log_{10} T_{1/2}^{\rm cal1}$ and experimental data $\log_{10} T_{1/2}^{\rm exp}$ to extract experimental α-particle preformation factors, which are denoted as $P_\alpha^{\rm exp}$. In the next step, we employ Eq. (21) and parameters in Table I to calculate α-particle preformation factors, which are denoted as $P_\alpha^{\rm Eq}$. $P_\alpha^{\rm exp}$, and $P_\alpha^{\rm Eq}$ and are also listed in Tables II–IV. From these tables, we can see that $P_\alpha^{\rm Eq}$ values are consistent with $P_\alpha^{\rm exp}$ data. In order to measure the agreements of estimated α-particle preformation factors by Eq. (21) with extracted experimental ones by Eq. (20), the standard deviations for all 535 nuclei, including 159 even-even nuclei, 295 odd-A nuclei, and 81 doubly odd nuclei, are calculated by

$$\sigma = \sqrt{\frac{1}{n}\sum \left(\log_{10} P_\alpha^{\rm Eq} - \log_{10} P_\alpha^{\rm exp}\right)^2}. \tag{22}$$

The results of standard deviations are listed in the last column of Table I. In this table, we can find that values of σ are satisfactory. For even-even nuclei, odd-A nuclei, and doubly odd nuclei, $P_\alpha^{\rm Eq}$ can well reproduce $P_\alpha^{\rm exp}$ within factors of $10^{0.213} = 1.63$, $10^{0.285} = 1.93$, and $10^{0.231} = 1.70$, respectively. Note that Eq. (21) not only is user friendly, but also can reproduce extracted experimental α-particle preformation factor with high precision.

Two types of α-particle preformation factors, $P_\alpha^{\rm exp}$ given by Eq. (20) and $P_\alpha^{\rm Eq}$ obtained from Eq. (21), for even-even, odd-A, and doubly odd nuclei are plotted as open dark and solid red circles in Figs. 1–3, respectively. From these figures, one can see that $P_\alpha^{\rm Eq}$ can fit $P_\alpha^{\rm exp}$ well, indicating that the

TABLE II. Calculations of α-particle preformation factors and α decay half-lives for even-even nuclei. Experimental α decay half-lives are taken from the latest evaluated nuclear properties table NUBASE2016 [83]. The α decay energies are taken from the latest evaluated atomic mass table AME2016 [84,85]. The α decay energies and half-lives are in units of MeV and s, respectively.

α transition		Q_α	l_{min}	$\log_{10} T_{1/2}^{exp}$	$\log_{10} T_{1/2}^{cal1}$	P_α^{exp}	P_α^{Eq}	$\log_{10} T_{1/2}^{cal2}$
^{148}Gd	^{144}Sm	3.27	0	9.35	8.68	0.2157	0.2223	9.34
^{150}Gd	^{146}Sm	2.81	0	13.75	13.17	0.2605	0.2829	13.72
^{150}Dy	^{146}Gd	4.35	0	3.07	2.17	0.125	0.1345	3.04
^{152}Dy	^{148}Gd	3.73	0	6.93	6.26	0.2145	0.1617	7.05
^{154}Dy	^{150}Gd	2.95	0	13.98	13.17	0.1557	0.2376	13.79
^{152}Er	^{148}Dy	4.94	0	1.06	0.12	0.1149	0.1215	1.03
^{154}Er	^{150}Dy	4.28	0	4.68	3.72	0.1115	0.1379	4.58
^{156}Er	^{152}Dy	3.48	0	10.24	9.49	0.1797	0.1799	10.24
^{154}Yb	^{150}Er	5.47	0	−0.35	−1.39	0.0926	0.117	−0.46
^{156}Yb	^{152}Er	4.81	0	2.41	1.79	0.2428	0.1266	2.69
^{158}Yb	^{154}Er	4.17	0	6.63	5.52	0.0785	0.1413	6.37
^{156}Hf	^{152}Yb	6.03	0	−1.63	−2.73	0.0796	0.116	−1.79
^{158}Hf	^{154}Yb	5.41	0	0.35	−0.18	0.2989	0.1193	0.75
^{160}Hf	^{156}Yb	4.9	0	3.28	2.28	0.1016	0.1212	3.2
^{162}Hf	^{158}Yb	4.42	0	5.69	5.07	0.242	0.1249	5.97
^{158}W	^{154}Hf	6.62	0	−2.9	−4.04	0.0729	0.1172	−3.11
^{160}W	^{156}Hf	6.07	0	−0.99	−2.05	0.0877	0.1153	−1.11
^{162}W	^{158}Hf	5.68	0	0.42	−0.46	0.1305	0.1108	0.49
^{164}W	^{160}Hf	5.28	0	2.22	1.31	0.1249	0.1075	2.28
^{166}W	^{162}Hf	4.86	0	4.74	3.49	0.0567	0.1059	4.47
^{168}W	^{164}Hf	4.5	0	6.2	5.57	0.2327	0.1034	6.55
^{180}W	^{176}Hf	2.52	0	25.75	24.54	0.061	0.1126	25.49
^{162}Os	^{158}W	6.77	0	−2.68	−3.76	0.0831	0.1147	−2.82
^{166}Os	^{162}W	6.14	0	−0.53	−1.55	0.0944	0.1001	−0.56
^{168}Os	^{164}W	5.82	0	0.68	−0.23	0.1229	0.0942	0.8
^{170}Os	^{166}W	5.54	0	1.89	1.01	0.1313	0.0881	2.06
^{172}Os	^{168}W	5.22	0	3.23	2.46	0.168	0.0834	3.54
^{174}Os	^{170}W	4.87	0	5.25	4.35	0.1245	0.0799	5.44
^{186}Os	^{182}W	2.82	0	22.8	21.72	0.0823	0.074	22.85
^{166}Pt	^{162}Os	7.29	0	−3.52	−4.73	0.0627	0.1065	−3.75
^{168}Pt	^{164}Os	6.99	0	−2.69	−3.78	0.0815	0.0984	−2.78
^{172}Pt	^{168}Os	6.46	0	−1	−2.02	0.0945	0.0836	−0.95
^{174}Pt	^{170}Os	6.18	0	0.06	−0.95	0.0961	0.0774	0.16
^{176}Pt	^{172}Os	5.89	0	1.2	0.28	0.1207	0.0721	1.42
^{178}Pt	^{174}Os	5.57	0	2.43	1.63	0.1584	0.0674	2.8
^{180}Pt	^{176}Os	5.24	0	4.27	3.28	0.1019	0.0635	4.48
^{182}Pt	^{178}Os	4.95	0	5.62	4.83	0.16	0.0596	6.05
^{184}Pt	^{180}Os	4.6	0	7.77	6.94	0.1474	0.0568	8.18
^{190}Pt	^{186}Os	3.27	0	19.31	17.86	0.0354	0.0557	19.12
^{172}Hg	^{168}Pt	7.53	0	−3.64	−4.79	0.0696	0.092	−3.76
^{174}Hg	^{170}Pt	7.23	0	−2.7	−3.9	0.0628	0.0845	−2.83
^{176}Hg	^{172}Pt	6.9	0	−1.65	−2.79	0.0729	0.0781	−1.68
^{178}Hg	^{174}Pt	6.58	0	−0.53	−1.69	0.0678	0.0722	−0.55
^{180}Hg	^{176}Pt	6.26	0	0.73	−0.47	0.063	0.0668	0.7
^{182}Hg	^{178}Pt	6	0	1.89	0.62	0.0533	0.0616	1.83
^{184}Hg	^{180}Pt	5.66	0	3.44	2.12	0.0474	0.0574	3.36
^{186}Hg	^{182}Pt	5.2	0	5.7	4.37	0.047	0.0546	5.64
^{178}Pb	^{174}Hg	7.79	0	−3.64	−4.94	0.0504	0.0796	−3.84
^{180}Pb	^{176}Hg	7.42	0	−2.39	−3.81	0.0374	0.0733	−2.68
^{184}Pb	^{180}Hg	6.77	0	−0.21	−1.64	0.0376	0.0618	−0.43
^{186}Pb	^{182}Hg	6.47	0	1.07	−0.54	0.0243	0.0568	0.7
^{188}Pb	^{184}Hg	6.11	0	2.43	0.94	0.0326	0.0526	2.22
^{190}Pb	^{186}Hg	5.7	0	4.24	2.81	0.0368	0.049	4.12
^{192}Pb	^{188}Hg	5.22	0	6.55	5.26	0.0522	0.0462	6.6
^{186}Po	^{182}Pb	8.5	0	−4.47	−6.36	0.0129	0.0603	−5.14
^{190}Po	^{186}Pb	7.69	0	−2.61	−4.08	0.0337	0.0508	−2.79

TABLE II. (*Continued.*)

α transition		Q_α	l_{min}	$\log_{10} T_{1/2}^{exp}$	$\log_{10} T_{1/2}^{cal1}$	P_α^{exp}	P_α^{Eq}	$\log_{10} T_{1/2}^{cal2}$
^{194}Po	^{190}Pb	6.99	0	−0.41	−1.79	0.0416	0.0426	−0.42
^{196}Po	^{192}Pb	6.66	0	0.75	−0.58	0.0467	0.0391	0.83
^{198}Po	^{194}Pb	6.31	0	2.27	0.82	0.0358	0.0359	2.27
^{200}Po	^{196}Pb	5.98	0	3.79	2.26	0.0293	0.0329	3.74
^{202}Po	^{198}Pb	5.7	0	5.14	3.53	0.0243	0.0302	5.05
^{204}Po	^{200}Pb	5.49	0	6.27	4.61	0.0216	0.0275	6.17
^{206}Po	^{202}Pb	5.33	0	7.14	5.44	0.02	0.025	7.05
^{208}Po	^{204}Pb	5.22	0	7.96	6.06	0.0124	0.0226	7.7
^{212}Po	^{208}Pb	8.95	0	−6.53	−8	0.034	0.0678	−6.83
^{214}Po	^{210}Pb	7.83	0	−3.79	−4.94	0.0699	0.0933	−3.91
^{216}Po	^{212}Pb	6.91	0	−0.84	−1.86	0.0961	0.1281	−0.96
^{218}Po	^{214}Pb	6.12	0	2.27	1.28	0.1037	0.1771	2.04
^{194}Rn	^{190}Po	7.86	0	−3.11	−3.9	0.1596	0.0494	−2.6
^{196}Rn	^{192}Po	7.62	0	−2.33	−3.16	0.1465	0.0448	−1.81
^{200}Rn	^{196}Po	7.04	0	0.07	−1.22	0.0509	0.0371	0.21
^{202}Rn	^{198}Po	6.77	0	1.09	−0.27	0.0433	0.0337	1.2
^{204}Rn	^{200}Po	6.55	0	2.01	0.61	0.0395	0.0306	2.12
^{206}Rn	^{202}Po	6.38	0	2.74	1.27	0.0343	0.0277	2.83
^{208}Rn	^{204}Po	6.26	0	3.37	1.79	0.0265	0.0251	3.39
^{210}Rn	^{206}Po	6.16	0	3.95	2.16	0.0161	0.0227	3.8
^{212}Rn	^{208}Po	6.38	0	3.16	1.15	0.0097	0.0203	2.84
^{214}Rn	^{210}Po	9.21	0	−6.57	−7.97	0.0401	0.0583	−6.73
^{216}Rn	^{212}Po	8.2	0	−4.35	−5.3	0.1108	0.076	−4.18
^{218}Rn	^{214}Po	7.26	0	−1.47	−2.37	0.1252	0.1017	−1.38
^{220}Rn	^{216}Po	6.41	0	1.75	0.92	0.1497	0.1405	1.77
^{222}Rn	^{218}Po	5.59	0	5.52	4.76	0.173	0.2041	5.45
^{202}Ra	^{198}Rn	7.88	0	−2.39	−3.34	0.1118	0.039	−1.93
^{204}Ra	^{200}Rn	7.64	0	−1.22	−2.58	0.0439	0.0353	−1.13
^{208}Ra	^{204}Rn	7.27	0	0.1	−1.37	0.0334	0.0289	0.17
^{214}Ra	^{210}Rn	7.27	0	0.39	−1.49	0.0133	0.0212	0.19
^{216}Ra	^{212}Rn	9.53	0	−6.74	−8.08	0.0462	0.0496	−6.77
^{218}Ra	^{214}Rn	8.55	0	−4.6	−5.61	0.0967	0.0628	−4.41
^{220}Ra	^{216}Rn	7.59	0	−1.75	−2.71	0.1079	0.0826	−1.63
^{222}Ra	^{218}Rn	6.68	0	1.53	0.65	0.1326	0.1135	1.59
^{224}Ra	^{220}Rn	5.79	0	5.5	4.7	0.1585	0.166	5.48
^{226}Ra	^{222}Rn	4.87	0	10.7	10.04	0.2181	0.2745	10.6
^{208}Th	^{204}Ra	8.2	0	−2.62	−3.65	0.0933	0.034	−2.18
^{212}Th	^{208}Ra	7.96	0	−1.5	−2.98	0.0327	0.0277	−1.43
^{214}Th	^{210}Ra	7.83	0	−1.06	−2.58	0.03	0.025	−0.98
^{216}Th	^{212}Ra	8.07	0	−1.59	−3.41	0.0151	0.0226	−1.76
^{218}Th	^{214}Ra	9.85	0	−6.93	−8.21	0.0527	0.0423	−6.84
^{220}Th	^{216}Ra	8.95	0	−5.01	−6.04	0.0946	0.0515	−4.75
^{222}Th	^{218}Ra	8.13	0	−2.65	−3.69	0.0911	0.0635	−2.49
^{224}Th	^{220}Ra	7.3	0	0.02	−0.93	0.1142	0.0813	0.16
^{226}Th	^{222}Ra	6.45	0	3.27	2.46	0.157	0.1101	3.42
^{228}Th	^{224}Ra	5.52	0	7.78	7.04	0.1806	0.1674	7.81
^{230}Th	^{226}Ra	4.77	0	12.38	11.74	0.2319	0.2544	12.34
^{216}U	^{212}Th	8.53	0	−2.16	−4.05	0.0129	0.0269	−2.48
^{218}U	^{214}Th	8.78	0	−3.26	−4.81	0.0284	0.0244	−3.19
^{222}U	^{218}Th	9.48	0	−5.33	−6.74	0.0384	0.0415	−5.36
^{224}U	^{220}Th	8.63	0	−3.4	−4.48	0.0844	0.0503	−3.18
^{226}U	^{222}Th	7.7	0	−0.57	−1.56	0.1015	0.0647	−0.37
^{230}U	^{226}Th	5.99	0	6.24	5.48	0.1727	0.1191	6.4
^{232}U	^{228}Th	5.41	0	9.34	8.64	0.201	0.1547	9.45
^{234}U	^{230}Th	4.86	0	12.89	12.22	0.2131	0.208	12.9
^{236}U	^{232}Th	4.57	0	14.87	14.21	0.2207	0.2433	14.83
^{228}Pu	^{224}U	7.94	0	0.32	−1.65	0.0106	0.0548	−0.39
^{230}Pu	^{226}U	7.18	0	2.01	1.08	0.1177	0.0685	2.24

TABLE II. (*Continued*.)

α transition		Q_α	$l_{\min}$	$\log_{10} T_{1/2}^{\text{exp}}$	$\log_{10} T_{1/2}^{\text{cal1}}$	P_α^{exp}	P_α^{Eq}	$\log_{10} T_{1/2}^{\text{cal2}}$
^{232}Pu	^{228}U	6.72	0	4.24	2.98	0.0548	0.0791	4.08
^{234}Pu	^{230}U	6.31	0	5.72	4.82	0.1252	0.0906	5.86
^{236}Pu	^{232}U	5.87	0	7.96	6.98	0.1056	0.1073	7.95
^{238}Pu	^{234}U	5.59	0	9.44	8.49	0.1105	0.1191	9.41
^{240}Pu	^{236}U	5.26	0	11.32	10.52	0.1584	0.138	11.38
^{242}Pu	^{238}U	4.98	0	13.07	12.3	0.1695	0.1564	13.11
^{244}Pu	^{240}U	4.67	0	15.4	14.6	0.157	0.185	15.33
^{234}Cm	^{230}Pu	7.37	0	2.28	1.15	0.074	0.0569	2.4
^{236}Cm	^{232}Pu	7.07	0	3.35	2.26	0.082	0.0613	3.48
^{238}Cm	^{234}Pu	6.67	0	5.31	3.95	0.0434	0.0689	5.11
^{240}Cm	^{236}Pu	6.4	0	6.37	5.2	0.0681	0.0746	6.33
^{242}Cm	^{238}Pu	6.22	0	7.15	6.08	0.0854	0.0782	7.19
^{244}Cm	^{240}Pu	5.9	0	8.76	7.7	0.0876	0.0872	8.76
^{246}Cm	^{242}Pu	5.48	0	11.17	10.07	0.0785	0.1039	11.05
^{248}Cm	^{244}Pu	5.16	0	13.08	12.05	0.0945	0.119	12.98
^{238}Cf	^{234}Cm	8.13	0	1.02	−0.91	0.0117	0.0399	0.49
^{240}Cf	^{236}Cm	7.71	0	1.61	0.55	0.0867	0.0439	1.91
^{242}Cf	^{238}Cm	7.52	0	2.42	1.26	0.0696	0.0454	2.6
^{244}Cf	^{240}Cm	7.33	0	3.07	1.96	0.0792	0.047	3.29
^{246}Cf	^{242}Cm	6.86	0	5.11	3.84	0.0543	0.0536	5.11
^{248}Cf	^{244}Cm	6.36	0	7.46	6.16	0.0506	0.063	7.36
^{250}Cf	^{246}Cm	6.13	0	8.62	7.33	0.0518	0.0673	8.5
^{252}Cf	^{248}Cm	6.22	0	7.94	6.85	0.0825	0.0632	8.05
^{254}Cf	^{250}Cm	5.93	0	9.22	8.31	0.1221	0.0695	9.47
^{244}Fm	^{240}Cf	8.55	0	−0.11	−1.63	0.0303	0.0309	−0.12
^{248}Fm	^{244}Cf	8	0	1.56	0.18	0.0419	0.0341	1.65
^{252}Fm	^{248}Cf	7.15	0	4.96	3.39	0.027	0.0418	4.77
^{254}Fm	^{250}Cf	7.31	0	4.07	2.67	0.0404	0.0388	4.08
^{256}Fm	^{252}Cf	7.03	0	5.07	3.83	0.0586	0.0414	5.22
^{254}No	^{250}Fm	8.23	0	1.75	0.03	0.0187	0.0278	1.58
^{256}No	^{252}Fm	8.58	0	0.46	−1.18	0.0225	0.0249	0.42
^{258}No	^{254}Fm	8.15	0	2.08	0.24	0.0144	0.027	1.81
^{256}Rf	^{252}No	8.93	0	0.32	−1.55	0.0136	0.0215	0.12
^{258}Rf	^{254}No	9.19	0	−0.98	−2.4	0.0384	0.0198	−0.69
^{260}Rf	^{256}No	8.9	0	0.02	−1.53	0.0279	0.0206	0.15
^{260}Sg	^{256}Rf	9.9	0	−1.91	−3.77	0.0139	0.0158	−1.97
^{264}Hs	^{260}Sg	10.59	0	−2.97	−4.97	0.0099	0.0125	−3.07
^{268}Hs	^{264}Sg	9.63	0	0.15	−2.44	0.0026	0.0143	−0.59
^{270}Hs	^{266}Sg	9.07	0	0.95	−0.76	0.0195	0.0156	1.05
^{270}Ds	^{266}Hs	11.12	0	−3.69	−5.69	0.0099	0.0102	−3.7
^{286}Fl	^{282}Cn	10.37	0	−0.46	−2.8	0.0045	0.0086	−0.74
^{288}Fl	^{284}Cn	10.07	0	−0.12	−1.99	0.0135	0.0088	0.06
^{290}Lv	^{286}Fl	11.01	0	−2.1	−3.92	0.0151	0.0071	−1.77
^{292}Lv	^{288}Fl	10.78	0	−1.62	−3.36	0.0183	0.0071	−1.21
^{294}Og	^{290}Lv	11.84	0	−2.94	−5.36	0.0038	0.0057	−3.12

analytic formula for estimating the α-particle preformation factor is credible. In addition, we can find that the sequence of nuclei in the order of decreasing P_α^{exp} and P_α^{Eq} are even-even nuclei, odd-A nuclei, and doubly odd nuclei, which satisfy the variation tendencies of α-particle preformation factors obtained by different models [28,29,77–82]. Moreover, one can find that the closer the neutron number is to the magic number $N = 126$, the smaller P_α^{exp} and P_α^{Eq} are. When N is far from the neutron magic number $N = 126$, P_α^{exp} and P_α^{Eq} will increase as the neutron number deviates from $N = 126$ shell closure, until the neutron number approaches the next neutron closed shell. This indicates that the closer the neutron number is to the magic number, the more difficult it is for an α particle to form inside its parent nucleus because P_α represents the probability of an α-cluster formation inside its parent nucleus before emission. It is also shown that the microscopic shell structure information is reflected by the observation of P_α^{Eq} obtained from Eq. (21). Noticeably, when neutron numbers

TABLE III. Same as Table II, but for α decay of odd-A nuclei. Elements with upper suffixes "m", "n", "p", or "x" indicate assignments to excited isomeric states (defined as higher states with half-lives greater than 100 ns). Suffixes "p" also indicate nonisomeric levels, but used in the AME2016 [84,85].

α transition		Q_α	$l_{\min}$	$\log_{10} T_{1/2}^{\text{exp}}$	$\log_{10} T_{1/2}^{\text{cal1}}$	P_α^{exp}	P_α^{Eq}	$\log_{10} T_{1/2}^{\text{cal2}}$
^{149}Tb	^{145}Eu	4.08	2	4.95	3.68	0.0534	0.0669	4.85
^{151}Tb	^{147}Eu	3.5	2	8.82	7.76	0.0872	0.1226	8.68
^{151}Dy	^{147}Gd	4.18	0	4.28	3.19	0.0814	0.0768	4.3
^{153}Dy	^{149}Gd	3.56	0	8.39	7.54	0.14	0.1405	8.39
^{151}Ho	^{147}Tb^{m}	4.64	0	2.2	1.09	0.0773	0.0622	2.29
^{151}Ho^{m}	^{147}Tb	4.74	0	1.79	0.6	0.065	0.0569	1.84
^{153}Ho^{m}	^{149}Tb	4.12	0	5.47	4.14	0.0468	0.088	5.2
^{153}Er	^{149}Dy	4.8	0	1.84	0.78	0.0861	0.0583	2.01
^{155}Er	^{151}Dy	4.12	0	6.15	4.74	0.0394	0.0938	5.77
^{153}Tm	^{149}Ho	5.25	0	0.21	−0.87	0.0827	0.054	0.39
^{153}Tm^{m}	^{149}Ho^{m}	5.24	0	0.43	−0.85	0.0527	0.0542	0.42
^{155}Tm	^{151}Ho	4.57	0	3.38	2.55	0.1481	0.0778	3.66
^{155}Yb	^{151}Er	5.34	0	0.3	−0.8	0.0787	0.0554	0.45
^{157}Yb	^{153}Er	4.62	0	3.89	2.76	0.0745	0.0795	3.86
^{155}Lu	^{151}Tm	5.8	0	−1.12	−2.3	0.0654	0.0546	−1.04
^{155}Lu^{m}	^{151}Tm^{m}	5.73	0	−0.74	−2	0.0547	0.0571	−0.76
^{155}Lu^{n}	^{151}Tm	7.58	8	−2.57	−4.48	0.0123	0.0115	−2.54
^{157}Lu^{m}	^{153}Tm	5.13	0	1.89	0.64	0.0561	0.0701	1.79
^{157}Hf	^{153}Yb	5.89	0	−0.91	−2.22	0.0492	0.0572	−0.98
^{157}Ta^{n}	^{153}Lu	7.95	8	−2.77	−4.75	0.0104	0.0158	−2.95
^{159}Ta	^{155}Lu^{m}	5.66	0	0.48	−0.83	0.0493	0.0712	0.32
^{159}Ta^{m}	^{155}Lu	5.75	0	0.01	−1.19	0.063	0.0678	−0.02
^{159}W	^{155}Hf	6.45	0	−2	−3.46	0.0348	0.0632	−2.26
^{161}W	^{157}Hf	5.92	0	−0.25	−1.46	0.0626	0.0673	−0.28
^{163}W	^{159}Hf	5.52	0	1.27	0.24	0.0937	0.0684	1.4
^{159}Re^{m}	^{155}Ta	6.97	0	−3.54	−4.8	0.0557	0.0678	−3.63
^{161}Re^{m}	^{157}Ta^{m}	6.43	0	−1.8	−2.97	0.0671	0.0701	−1.82
^{163}Re	^{159}Ta	6.01	0	0.08	−1.41	0.0324	0.0697	−0.25
^{163}Re^{m}	^{159}Ta^{m}	6.07	0	−0.49	−1.63	0.0719	0.0679	−0.47
^{165}Re	^{161}Ta	5.69	0	1.25	−0.13	0.0418	0.067	1.04
^{165}Re^{m}	^{161}Ta^{m}	5.66	0	1.12	0.02	0.0781	0.0681	1.18
^{167}Re^{m}	^{163}Ta	5.41	0	2.77	1.17	0.0249	0.064	2.36
^{169}Re	^{165}Ta	5.01	3	5.18	3.79	0.0407	0.05	5.1
^{169}Re^{m}	^{165}Ta^{m}	5.16	3	3.88	3	0.1327	0.0459	4.34
^{161}Os	^{157}W	7.07	0	−3.19	−4.74	0.0284	0.0722	−3.6
^{163}Os	^{159}W	6.69	0	−2.26	−3.5	0.0578	0.069	−2.34
^{165}Os	^{161}W	6.34	0	−1.1	−2.28	0.0659	0.0656	−1.1
^{167}Os	^{163}W	5.99	0	0.21	−0.93	0.072	0.0629	0.27
^{169}Os	^{165}W	5.71	0	1.4	0.21	0.0652	0.0588	1.44
^{165}Ir^{m}	^{161}Re^{m}	6.89	0	−2.57	−3.82	0.0574	0.0703	−2.66
^{167}Ir	^{163}Re	6.51	0	−1.17	−2.51	0.0457	0.0668	−1.33
^{167}Ir^{m}	^{163}Re^{m}	6.56	0	−1.55	−2.71	0.0683	0.0655	−1.53
^{169}Ir	^{165}Re	6.14	0	−0.18	−1.13	0.1133	0.0636	0.07
^{169}Ir^{m}	^{165}Re^{m}	6.27	0	−0.45	−1.63	0.067	0.0606	−0.41
^{171}Ir	^{167}Re^{m}	5.87	0	1.31	−0.05	0.0439	0.0589	1.18
^{171}Ir^{m}	^{167}Re	6.16	2	0.43	−0.94	0.0421	0.0433	0.42
^{173}Ir^{m}	^{169}Re	5.94	2	1.26	−0.09	0.0448	0.0391	1.32
^{175}Ir	^{171}Re	5.43	2	3.02	2.23	0.1607	0.0403	3.62
^{177}Ir	^{173}Re	5.08	0	4.69	3.67	0.0959	0.0474	5
^{167}Pt	^{163}Os	7.16	0	−3.1	−4.33	0.0587	0.0705	−3.18
^{171}Pt	^{167}Os	6.61	0	−1.3	−2.54	0.0579	0.0582	−1.3
^{173}Pt	^{169}Os	6.36	0	−0.35	−1.64	0.0524	0.0526	−0.36
^{175}Pt	^{171}Os	6.16	2	0.58	−0.57	0.0709	0.0387	0.84
^{177}Pt	^{173}Os	5.64	0	2.27	1.36	0.1239	0.0472	2.68
^{179}Pt	^{175}Os	5.41	2	3.94	2.72	0.0595	0.0356	4.16

TABLE III. (*Continued.*)

α transition		Q_α	l_{min}	$\log_{10} T_{1/2}^{exp}$	$\log_{10} T_{1/2}^{cal1}$	P_α^{exp}	P_α^{Eq}	$\log_{10} T_{1/2}^{cal2}$
^{181}Pt	^{177}Os	5.15	0	4.85	3.74	0.0777	0.0399	5.14
^{183}Pt	^{179}Os	4.82	0	6.61	5.57	0.0914	0.0383	6.98
^{171}Au^m	^{167}Ir^m	7.16	0	−2.76	−4.04	0.0527	0.0642	−2.85
^{173}Au	^{169}Ir	6.84	0	−1.53	−2.96	0.0367	0.0588	−1.73
^{173}Au^m	^{169}Ir^m	6.9	0	−1.86	−3.17	0.0489	0.0578	−1.94
^{175}Au	^{171}Ir	6.59	0	−0.64	−2.08	0.0364	0.0529	−0.8
^{175}Au^m	^{171}Ir^m	6.59	0	−0.75	−2.08	0.0468	0.0529	−0.8
^{177}Au	^{173}Ir	6.3	0	0.56	−1	0.0277	0.0482	0.31
^{177}Au^m	^{173}Ir^m	6.26	0	0.25	−0.85	0.0786	0.0487	0.46
^{179}Au	^{175}Ir	5.98	1	1.51	0.35	0.0695	0.0399	1.75
^{181}Au	^{177}Ir	5.75	2	2.7	1.56	0.0734	0.0331	3.04
^{183}Au	^{179}Ir	5.47	0	3.89	2.59	0.0498	0.0369	4.02
^{185}Au	^{181}Ir	5.18	0	4.98	4.05	0.1167	0.0342	5.51
^{171}Hg	^{167}Pt	7.67	2	−4.15	−4.9	0.1808	0.0612	−3.68
^{173}Hg	^{169}Pt	7.38	2	−3.1	−4.04	0.1146	0.0549	−2.78
^{177}Hg	^{173}Pt	6.74	2	−0.82	−1.92	0.08	0.0452	−0.58
^{179}Hg	^{175}Pt	6.36	0	0.14	−0.87	0.098	0.0507	0.43
^{181}Hg	^{177}Pt	6.28	2	1.12	−0.27	0.0401	0.0358	1.17
^{183}Hg	^{179}Pt	6.04	0	1.9	0.42	0.0326	0.0389	1.83
^{185}Hg	^{181}Pt	5.77	0	2.91	1.58	0.0473	0.0352	3.03
^{177}Tl	^{173}Au	7.07	0	−1.61	−2.97	0.0432	0.0651	−1.79
^{177}Tl^m	^{173}Au^m	7.66	0	−3.44	−4.91	0.0343	0.0571	−3.66
^{179}Tl	^{175}Au	6.71	0	−0.36	−1.75	0.0407	0.0594	−0.52
^{179}Tl^m	^{175}Au^m	7.38	0	−2.85	−4.07	0.0607	0.0509	−2.77
^{181}Tl^m	^{177}Au^m	6.97	2	−0.46	−2.42	0.0109	0.0387	−1.01
^{183}Tl	^{179}Au	5.98	0	2.54	1.16	0.0422	0.0502	2.46
^{183}Tl^m	^{179}Au	6.61	3	0.54	−0.83	0.0429	0.0326	0.66
^{187}Tl^m	^{183}Au	5.66	2	4	2.87	0.0732	0.0317	4.37
^{179}Pb	^{175}Hg	7.6	2	−2.41	−4.06	0.0224	0.0522	−2.78
^{183}Pb^m	^{179}Hg	7.02	3	−0.38	−1.93	0.0283	0.0382	−0.51
^{185}Pb^m	^{181}Hg^m	6.56	0	0.91	−0.82	0.0187	0.0463	0.51
^{187}Pb	^{183}Hg	6.39	2	2.2	0.06	0.0072	0.0333	1.54
^{187}Pb^m	^{183}Hg^m	6.21	0	2.18	0.53	0.0223	0.0419	1.9
^{189}Pb	^{185}Hg	5.92	2	3.99	2.1	0.0128	0.0311	3.61
^{191}Pb^m	^{187}Hg^m	5.4	0	5.82	4.29	0.0297	0.0358	5.73
^{187}Bi	^{183}Tl	7.78	5	−1.43	−3.24	0.0154	0.0262	−1.66
^{187}Bi^m	^{183}Tl	7.89	0	−3.43	−5.02	0.0261	0.0394	−3.61
^{189}Bi	^{185}Tl	7.27	5	−0.18	−1.64	0.0351	0.0239	−0.01
^{191}Bi	^{187}Tl^m	6.45	0	1.36	−0.07	0.0374	0.0356	1.38
^{191}Bi^m	^{187}Tl	7.02	0	−0.78	−2.26	0.0327	0.0323	−0.77
^{193}Bi	^{189}Tl^m	6.02	0	3.26	1.68	0.0267	0.0325	3.17
^{193}Bi^m	^{189}Tl	6.61	0	0.56	−0.8	0.0439	0.0292	0.74
^{195}Bi	^{191}Tl^m	5.54	0	5.76	4.01	0.0178	0.0302	5.53
^{195}Bi^m	^{191}Tl	6.23	0	2.42	0.73	0.0207	0.0264	2.31
^{209}Bi	^{205}Tl	3.14	5	26.8	24.29	0.003	0.0107	26.26
^{211}Bi	^{207}Tl	6.75	5	2.11	−0.21	0.0048	0.0198	1.49
^{213}Bi	^{209}Tl	5.99	5	5.12	2.96	0.007	0.0215	4.63
^{187}Po	^{183}Pb	7.98	2	−2.85	−4.61	0.0175	0.0415	−3.23
^{189}Po	^{185}Pb	7.69	2	−2.42	−3.78	0.0439	0.0365	−2.34
^{195}Po	^{191}Pb	6.75	0	0.69	−0.89	0.0259	0.0305	0.62
^{195}Po^m	^{191}Pb^m	6.84	0	0.33	−1.26	0.0258	0.0301	0.26
^{197}Po	^{193}Pb	6.41	0	2.08	0.43	0.0225	0.0271	2
^{197}Po^m	^{193}Pb^m	6.51	0	1.48	0.02	0.0345	0.0267	1.59
^{199}Po	^{195}Pb	6.08	0	3.64	1.84	0.0159	0.0241	3.46
^{199}Po^m	^{195}Pb^m	6.18	0	3.02	1.36	0.022	0.0237	2.98
^{201}Po	^{197}Pb	5.8	0	4.92	3.05	0.0137	0.0213	4.73

TABLE III. (*Continued.*)

α transition		Q_α	l_{min}	$\log_{10} T_{1/2}^{exp}$	$\log_{10} T_{1/2}^{cal1}$	P_α^{exp}	P_α^{Eq}	$\log_{10} T_{1/2}^{cal2}$
$^{201}Po^m$	$^{197}Pb^m$	5.9	0	4.34	2.55	0.0162	0.0209	4.23
^{203}Po	^{199}Pb	5.5	2	6.29	4.86	0.037	0.0156	6.67
$^{203}Po^m$	^{199}Pb	6.14	5	5.05	2.92	0.0073	0.0112	4.87
^{205}Po	^{201}Pb	5.33	0	7.18	5.46	0.0191	0.0164	7.25
^{207}Po	^{203}Pb	5.22	0	7.99	6.06	0.0117	0.0141	7.91
^{209}Po	$^{205}Pb^m$	4.98	0	9.59	7.46	0.0073	0.0124	9.36
$^{211}Po^m$	^{207}Pb	9.06	13	1.4	−0.66	0.0087	0.0026	1.93
^{213}Po	^{209}Pb	8.54	0	−5.43	−6.94	0.0312	0.0444	−5.58
^{215}Po	^{211}Pb	7.53	0	−2.75	−3.99	0.0572	0.0479	−2.67
^{219}Po	^{215}Pb	5.92	0	3.34	2.19	0.0702	0.0568	3.43
^{191}At	$^{187}Bi^m$	7.71	0	−2.68	−3.77	0.0816	0.0476	−2.44
$^{191}At^m$	^{187}Bi	7.88	2	−2.66	−4	0.0457	0.0386	−2.58
^{193}At	$^{189}Bi^m$	7.39	0	−1.54	−2.76	0.0595	0.0419	−1.39
$^{193}At^m$	^{189}Bi	7.58	2	−1.68	−3.11	0.0371	0.0339	−1.64
$^{193}At^n$	^{189}Bi	7.62	3	−0.93	−2.93	0.0101	0.0312	−1.42
^{195}At	$^{191}Bi^m$	7.1	0	−0.54	−1.79	0.0561	0.0367	−0.35
^{197}At	^{193}Bi	7.11	0	−0.39	−1.84	0.0361	0.0311	−0.33
$^{197}At^m$	$^{193}Bi^m$	6.84	0	0.3	−0.87	0.0674	0.0321	0.62
^{199}At	^{195}Bi	6.78	0	0.89	−0.64	0.0291	0.0274	0.92
$^{199}At^m$	^{195}Bi	7.02	5	1.44	−0.12	0.0275	0.0174	1.64
^{201}At	^{197}Bi	6.47	0	2.07	0.51	0.027	0.0241	2.12
^{203}At	^{199}Bi	6.21	0	3.15	1.6	0.0282	0.021	3.28
^{205}At	^{201}Bi	6.02	0	4.3	2.45	0.014	0.0183	4.18
^{207}At	^{203}Bi	5.87	0	4.81	3.12	0.0201	0.0158	4.92
^{209}At	^{205}Bi	5.76	0	5.67	3.66	0.0097	0.0136	5.53
^{211}At	^{207}Bi	5.98	0	4.79	2.49	0.005	0.0113	4.44
^{213}At	^{209}Bi	9.25	0	−6.9	−8.4	0.032	0.0415	−7.02
^{215}At	^{211}Bi	8.18	0	−4	−5.6	0.0249	0.0444	−4.25
^{217}At	^{213}Bi	7.2	0	−1.49	−2.52	0.0933	0.0483	−1.2
^{219}At	^{215}Bi	6.34	0	1.78	0.74	0.0925	0.0531	2.02
^{193}Rn	^{189}Po	8.04	2	−2.94	−4.15	0.0618	0.0412	−2.76
^{195}Rn	^{191}Po	7.69	0	−2.15	−3.39	0.0586	0.0437	−2.03
$^{195}Rn^m$	$^{191}Po^m$	7.71	0	−2.22	−3.45	0.059	0.0436	−2.09
^{197}Rn	^{193}Po	7.41	0	−1.27	−2.49	0.0604	0.0381	−1.07
$^{197}Rn^m$	$^{193}Po^m$	7.51	0	−1.59	−2.82	0.059	0.0377	−1.4
^{203}Rn	^{199}Po	6.63	0	1.82	0.29	0.0293	0.025	1.89
$^{203}Rn^m$	$^{199}Po^m$	6.68	0	1.55	0.08	0.0333	0.0249	1.68
^{205}Rn	^{201}Po	6.39	2	2.84	1.57	0.0537	0.0179	3.31
^{207}Rn	^{203}Po	6.25	0	3.42	1.84	0.0267	0.0187	3.57
^{209}Rn	^{205}Po	6.16	0	4	2.25	0.0176	0.016	4.04
^{211}Rn	^{207}Po	5.97	2	5.28	3.34	0.0114	0.0114	5.28
^{213}Rn	^{209}Po	8.25	5	−1.71	−4.03	0.0048	0.0154	−2.22
^{215}Rn	^{211}Po	8.84	0	−5.64	−7.06	0.0382	0.0415	−5.67
^{217}Rn	^{213}Po	7.89	0	−3.27	−4.38	0.0767	0.0442	−3.03
^{219}Rn	^{215}Po	6.95	2	0.6	−0.95	0.0282	0.0288	0.59
^{221}Rn	^{217}Po	6.16	2	3.84	2.27	0.0266	0.0316	3.77
^{223}Rn	^{219}Po	5.28	2	8.56	6.73	0.0146	0.0368	8.16
^{197}Fr	$^{193}At^m$	7.88	0	−2.63	−3.64	0.0992	0.0463	−2.3
^{199}Fr	^{195}At	7.82	0	−2.18	−3.45	0.0537	0.0396	−2.05
$^{199}Fr^m$	$^{195}At^m$	7.83	0	−2.19	−3.51	0.0481	0.0396	−2.1
^{201}Fr	^{197}At	7.52	0	−1.2	−2.54	0.0462	0.0344	−1.07
$^{201}Fr^m$	$^{197}At^m$	7.6	0	−1.77	−2.81	0.0909	0.0342	−1.34
^{203}Fr	^{199}At	7.27	0	−0.26	−1.73	0.0341	0.0297	−0.2
$^{203}Fr^m$	$^{199}At^m$	7.39	0	−0.68	−2.14	0.0347	0.0295	−0.61
^{205}Fr	^{201}At	7.05	0	0.58	−0.95	0.0292	0.0257	0.64
^{207}Fr	^{203}At	6.89	0	1.19	−0.37	0.0276	0.0221	1.29
^{209}Fr	^{205}At	6.78	0	1.75	0.06	0.0203	0.019	1.78
^{211}Fr	^{207}At	6.66	0	2.33	0.45	0.0131	0.0163	2.23

TABLE III. (*Continued.*)

α transition		Q_α	l_{min}	$\log_{10} T_{1/2}^{exp}$	$\log_{10} T_{1/2}^{cal1}$	P_α^{exp}	P_α^{Eq}	$\log_{10} T_{1/2}^{cal2}$
^{213}Fr	^{209}At	6.91	0	1.54	−0.53	0.0085	0.0139	1.32
^{215}Fr	^{211}At	9.54	0	−7.07	−8.42	0.044	0.0388	−7.01
^{219}Fr	^{215}At	7.45	0	−1.7	−2.62	0.1193	0.0452	−1.28
^{221}Fr	^{217}At	6.46	2	2.46	1.43	0.0928	0.0304	2.94
^{223}Fr	^{219}At	5.56	4	7.34	6.36	0.1047	0.023	8
^{201}Ra	^{197}Rn	8	0	−1.7	−3.7	0.01	0.0422	−2.32
^{201}Ra^{m}	^{197}Rn^{m}	8.07	0	−2.22	−3.89	0.0212	0.0421	−2.52
^{203}Ra	^{199}Rn	7.74	0	−1.44	−2.89	0.0359	0.0364	−1.45
^{203}Ra^{m}	^{199}Rn^{m}	7.76	0	−1.6	−2.98	0.0419	0.0364	−1.54
^{207}Ra	^{203}Rn	7.27	2	0.21	−1.06	0.0547	0.0223	0.6
^{209}Ra	^{205}Rn	7.14	0	0.67	−0.91	0.0259	0.0232	0.72
^{213}Ra	^{209}Rn	6.86	2	2.31	0.35	0.011	0.0141	2.2
^{215}Ra	^{211}Rn	8.86	5	−2.78	−5.09	0.0048	0.0137	−3.23
^{217}Ra	^{213}Rn	9.16	0	−5.79	−7.22	0.0371	0.0386	−5.8
^{219}Ra	^{215}Rn	8.14	2	−2	−4.17	0.0068	0.0247	−2.56
^{221}Ra	^{217}Rn	6.88	2	1.45	0.14	0.049	0.0286	1.68
^{223}Ra	^{219}Rn	5.98	2	5.99	4.04	0.0112	0.0325	5.53
^{205}Ac	^{201}Fr^{n}	7.9	3	−1.1	−2.48	0.0411	0.0296	−0.95
^{207}Ac	^{203}Fr	7.85	0	−1.51	−2.92	0.0392	0.0332	−1.44
^{211}Ac	^{207}Fr	7.62	0	−0.67	−2.25	0.0262	0.0244	−0.64
^{215}Ac	^{211}Fr	7.75	0	−0.77	−2.73	0.0109	0.018	−0.99
^{217}Ac	^{213}Fr	9.83	0	−7.16	−8.45	0.0513	0.0363	−7.01
^{217}Ac^{m}	^{213}Fr	11.84	11	−4.77	−7.07	0.0049	0.0026	−4.49
^{219}Ac	^{215}Fr	8.83	0	−4.93	−6.04	0.0775	0.0382	−4.62
^{221}Ac	^{217}Fr	7.78	0	−1.28	−2.95	0.0215	0.0416	−1.57
^{223}Ac	^{219}Fr	6.78	2	2.1	0.93	0.0664	0.0278	2.48
^{225}Ac	^{221}Fr	5.94	2	5.93	4.72	0.0613	0.0313	6.23
^{227}Ac	^{223}Fr	5.04	0	10.7	9.38	0.0488	0.063	10.59
^{209}Th^{m}	^{205}Ra^{m}	8.28	0	−2.51	−3.91	0.0401	0.0354	−2.45
^{215}Th	^{211}Ra	7.67	2	0.08	−1.79	0.0136	0.0185	−0.05
^{217}Th	^{213}Ra	9.44	5	−3.61	−5.9	0.005	0.0123	−3.99
^{219}Th	^{215}Ra	9.51	0	−5.99	−7.44	0.0354	0.0356	−5.99
^{221}Th	^{217}Ra	8.63	2	−2.75	−4.87	0.0075	0.0222	−3.22
^{223}Th	^{219}Ra	7.57	2	−0.22	−1.6	0.0423	0.0245	0.02
^{225}Th	^{221}Ra	6.92	2	2.77	0.78	0.0104	0.0257	2.37
^{227}Th	^{223}Ra	6.15	2	6.21	4.08	0.0075	0.0283	5.63
^{229}Th	^{225}Ra	5.17	2	11.4	9.4	0.0101	0.0346	10.86
^{231}Th	^{227}Ra	4.21	2	17.36	16.34	0.0959	0.0458	17.68
^{213}Pa	^{209}Ac	8.4	0	−2.15	−3.97	0.0154	0.0327	−2.48
^{215}Pa	^{211}Ac	8.24	0	−1.85	−3.52	0.0217	0.028	−1.96
^{217}Pa	^{213}Ac	8.49	0	−2.46	−4.31	0.014	0.0243	−2.7
^{221}Pa	^{217}Ac	9.25	0	−5.23	−6.48	0.0565	0.0349	−5.02
^{223}Pa	^{219}Ac	8.33	0	−2.29	−3.93	0.0228	0.0369	−2.5
^{227}Pa	^{223}Ac	6.58	0	3.43	2.29	0.0718	0.044	3.64
^{229}Pa	^{225}Ac	5.84	1	7.43	5.91	0.0302	0.0364	7.35
^{219}U	^{215}Th	9.94	5	−4.26	−6.51	0.0056	0.0111	−4.55
^{221}U	^{217}Th	9.89	0	−6.18	−7.68	0.0314	0.0328	−6.2
^{225}U	^{221}Th	8.02	2	−1.21	−2.34	0.0755	0.022	−0.68
^{227}U	^{223}Th	7.23	2	1.82	0.34	0.0333	0.0235	1.97
^{229}U	^{225}Th	6.48	0	4.24	3.17	0.0863	0.0428	4.54
^{231}U	^{227}Th	5.58	2	9.95	7.99	0.0109	0.03	9.51
^{233}U	^{229}Th	4.91	0	12.7	11.87	0.1469	0.0578	13.11
^{227}Np	^{223}Pa	7.82	2	−0.29	−1.34	0.0894	0.0215	0.33
^{229}Np	^{225}Pa	7.02	1	2.55	1.41	0.0733	0.029	2.95
^{231}Np	^{227}Pa	6.36	1	5.14	4.22	0.1188	0.0311	5.73
^{235}Np	^{231}Pa	5.19	1	12.12	10.52	0.025	0.0372	11.95
^{237}Np	^{233}Pa	4.96	1	13.83	12.07	0.0173	0.0374	13.5
^{239}Np	^{235}Pa	4.6	1	16.61	14.68	0.0117	0.0397	16.08

TABLE III. (*Continued.*)

α transition		Q_α	l_{min}	$\log_{10} T_{1/2}^{exp}$	$\log_{10} T_{1/2}^{cal1}$	P_α^{exp}	P_α^{Eq}	$\log_{10} T_{1/2}^{cal2}$
^{231}Pu	^{227}U	6.84	0	3.58	2.46	0.0756	0.0384	3.88
^{233}Pu	^{229}U	6.41	2	6	4.61	0.0406	0.0235	6.24
^{235}Pu	^{231}U	5.95	0	7.72	6.55	0.0663	0.041	7.93
^{239}Pu	^{235}U^{xm}	5.24	0	11.88	10.6	0.0518	0.0436	11.96
^{241}Pu	^{237}U	5.14	2	13.26	11.54	0.0189	0.025	13.14
^{229}Am	^{225}Np	8.14	2	0.3	−1.67	0.0109	0.0197	0.04
^{233}Am	^{229}Np	7.06	1	3.62	2.07	0.0279	0.0258	3.66
^{235}Am	^{231}Np	6.59	1	5.18	4.01	0.067	0.0266	5.58
^{237}Am	^{233}Np	6.2	1	7.24	5.84	0.04	0.0271	7.41
^{239}Am	^{235}Np	5.92	1	8.63	7.24	0.0406	0.0271	8.8
^{241}Am	^{237}Np	5.64	1	10.14	8.8	0.0466	0.0272	10.37
^{243}Am	^{239}Np	5.44	1	11.37	9.96	0.0397	0.0269	11.53
^{233}Cm	^{229}Pu	7.47	0	2.13	0.78	0.0453	0.0327	2.27
^{237}Cm	^{233}Pu	6.78	0	4.82	3.5	0.0469	0.0325	4.98
^{241}Cm	^{237}Pu	6.19	3	8.45	6.78	0.0217	0.0156	8.59
^{243}Cm	^{239}Pu	6.17	2	8.96	6.57	0.0041	0.0179	8.32
^{245}Cm	^{241}Pu	5.62	2	11.42	9.46	0.011	0.0194	11.17
^{247}Bk	^{243}Am	5.89	2	10.64	8.43	0.0061	0.0171	10.19
^{241}Cf	^{237}Cm^{p}	7.46	0	2.75	1.51	0.057	0.0251	3.11
^{243}Cf	^{239}Cm	7.42	3	3.66	2.16	0.0312	0.0113	4.1
^{245}Cf	^{241}Cm	7.26	0	3.87	2.18	0.0204	0.0225	3.83
^{247}Cf	^{243}Cm	6.5	2	7.5	5.78	0.0189	0.0148	7.61
^{251}Cf	^{247}Cm	6.18	5	10.45	8.38	0.0085	0.0074	10.51
^{245}Es	^{241}Bk^{p}	7.87	0	2.22	0.28	0.0115	0.0203	1.97
^{247}Es	^{243}Bk^{p}	7.44	1	3.59	1.93	0.0219	0.0152	3.75
^{249}Es	^{245}Bk^{p}	6.9	1	6.03	4.2	0.0149	0.0159	6
^{253}Es	^{249}Bk	6.74	0	6.25	4.77	0.0331	0.0191	6.49
^{255}Es	^{251}Bk^{m}	6.4	0	7.63	6.3	0.0467	0.0193	8.01
^{243}Fm	^{239}Cf	8.7	1	−0.6	−1.98	0.0417	0.0143	−0.13
^{247}Fm	^{243}Cf	8.26	4	1.69	0.13	0.0278	0.0069	2.29
^{247}Fm^{m}	^{243}Cf	8.31	0	0.76	−0.88	0.0228	0.0176	0.87
^{253}Fm	^{249}Cf^{m}	7.05	2	6.33	4.07	0.0055	0.0108	6.04
^{257}Fm	^{253}Cf	6.86	2	6.94	4.81	0.0074	0.0097	6.82
^{247}Md	^{243}Es	8.77	1	0.08	−1.91	0.0103	0.0123	0.001
^{247}Md^{m}	^{243}Es	9.03	3	−0.5	−2.29	0.0164	0.0077	−0.18
^{251}Md	^{247}Es	7.96	1	3.4	0.73	0.0021	0.0122	2.64
^{251}No	^{247}Fm	8.76	0	−0.02	−1.65	0.0232	0.0145	0.19
^{251}No^{m}	^{247}Fm^{m}	8.82	0	0.01	−1.84	0.0142	0.0143	0.01
^{253}No	^{249}Fm	8.42	1	2.23	−0.48	0.0019	0.0106	1.49
^{255}No	^{251}Fm^{m}	8.23	2	2.84	0.26	0.0026	0.0082	2.35
^{259}No	^{255}Fm	7.85	2	3.66	1.56	0.0078	0.0075	3.68
^{253}Lr	^{249}Md	8.93	0	−0.15	−1.84	0.0204	0.0132	0.04
^{253}Lr^{m}	^{249}Md^{m}	8.86	0	0.17	−1.62	0.0162	0.0134	0.25
^{255}Lr	^{251}Md^{p}	8.5	0	1.49	−0.54	0.0092	0.0132	1.34
^{257}Lr	^{253}Md	9.08	4	0.78	−1.58	0.0044	0.0043	0.79
^{259}Lr	^{255}Md^{p}	8.58	0	0.9	−0.83	0.0185	0.0112	1.12
^{255}Rf	^{251}No	9.06	1	0.54	−1.86	0.0041	0.0091	0.19
^{257}Rf^{m}	^{253}No	9.16	2	0.69	−2.03	0.0019	0.0066	0.15
^{259}Rf	^{255}No^{p}	9.03	0	0.46	−1.9	0.0044	0.0105	0.08
^{261}Rf	^{257}No	8.65	0	0.9	−0.72	0.0237	0.0104	1.26
^{263}Rf	^{259}No	8.26	4	3.34	1.36	0.0105	0.0041	3.75
^{259}Db	^{255}Lr^{m}	9.58	1	−0.29	−3.11	0.0015	0.0073	−0.97
^{259}Sg	^{255}Rf	9.77	2	−0.38	−3.14	0.0017	0.0058	−0.9
^{259}Sg^{m}	^{255}Rf^{m}	9.71	2	−0.63	−2.97	0.0046	0.0058	−0.74
^{261}Sg	^{257}Rf	9.71	2	−0.73	−3.02	0.0051	0.0054	−0.75
^{263}Sg	^{259}Rf	9.41	0	0.03	−2.41	0.0036	0.0087	−0.35
^{261}Bh	^{257}Db	10.5	3	−1.87	−4.53	0.0022	0.0039	−2.12

TABLE III. (*Continued.*)

α transition		Q_α	l_{min}	$\log_{10} T_{1/2}^{exp}$	$\log_{10} T_{1/2}^{cal1}$	P_α^{exp}	P_α^{Eq}	$\log_{10} T_{1/2}^{cal2}$
^{265}Hs	^{261}Sg	10.47	0	−2.71	−4.7	0.0102	0.0071	−2.55
^{269}Hs	^{265}Sg	9.35	0	1.2	−1.62	0.0015	0.0072	0.53
^{267}Ds	^{263}Hs	11.78	0	−5	−7.1	0.008	0.0057	−4.85
^{269}Ds	^{265}Hs^m	11.28	0	−3.64	−6.04	0.004	0.0056	−3.79
^{271}Ds	^{267}Hs	10.88	5	−1.05	−4.01	0.0011	0.0017	−1.24
^{271}Ds^m	^{267}Hs	10.95	2	−2.77	−5.08	0.0049	0.0032	−2.59
^{273}Ds	^{269}Hs	11.38	3	−3.62	−5.92	0.005	0.0023	−3.28
^{277}Ds	^{273}Hs	10.83	4	−2.22	−4.39	0.0068	0.0017	−1.62
^{277}Cn	^{273}Ds^m	11.42	0	−3.07	−5.9	0.0015	0.0041	−3.51
^{281}Cn	^{277}Ds	10.46	4	−0.74	−2.87	0.0075	0.0016	−0.08
^{289}Fl	^{285}Cn	9.97	0	0.38	−1.72	0.008	0.0033	0.77

enter the superheavy nuclei regions, P_α^{exp} and P_α^{Eq} still decrease while neutron number increases, which is consistent with the decreasing trends of α-particle preformation factors when the neutron numbers approach $N = 126$ closed shells. This means that both P_α^{exp} and P_α^{Eq} obtained by Eq. (21) provide positive signals for the existence of an island of stability for superheavy nuclei.

For a detailed comparison, the α-particle preformation factors extracted from Eq. (20) and estimated by Eq. (21) for Th isotopes are plotted as open dark and solid red circles in Fig. 4. From this figure, we can find that P_α^{Eq} can well reproduce P_α^{exp}. The closer the neutron number is to $N = 126$, the smaller the α-particle preformation factor is. In addition, it is clear that, with the change of neutron number, α-particle preformation factors show the periodic odd-even staggering effect, and this effect becomes more significant after neutron number crosses the $N = 126$ shell closure. Moreover, P_α^{exp} and P_α^{Eq} of odd-A nuclei are less than that of neighboring even-even nuclei, indicating that the presence of an odd nucleon will inhibit the formation of an α cluster inside its parent nucleus. Therefore, Eq. (21) can correctly reflect microscopic nuclear structure information such as the shell effect and the odd-even staggering effect.

The calculations of α decay half-lives with the α-particle preformation factors obtained by Eq. (21), P_α^{Eq}, in GLDM are performed, which are denoted as $\log_{10} T_{1/2}^{cal2}$ and are listed in Tables II–IV for even-even nuclei, odd-A nuclei, and doubly odd nuclei, respectively. In these three tables, the first four columns represent α decay parent nucleus, daughter nucleus, experimental α decay energy, and the minimum angular momentum carried by the α-particle, while the spin and parity values for α decay parent and daughter nuclei are taken from the latest evaluated nuclear properties table NUBASE2016 [83]. The fifth column is the experimental α decay half-life. The sixth column represents the calculated α decay half-life within GLDM with $P_\alpha = 1$. The seventh column is the extracted experimental α-particle preformation factor using

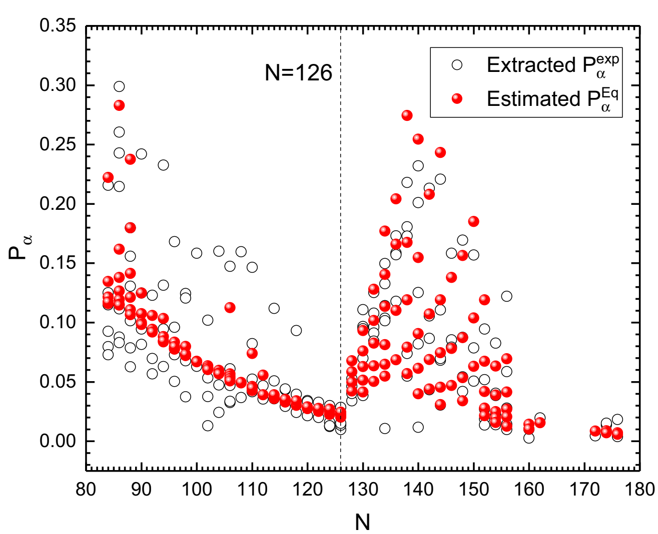

FIG. 1. The extracted experimental α-particle preformation factor P_α^{exp} from Eq. (20) and the estimated one P_α^{Eq} by Eq. (21) of even-even nuclei. The open dark and solid red circles denote P_α^{exp} and P_α^{Eq}, respectively.

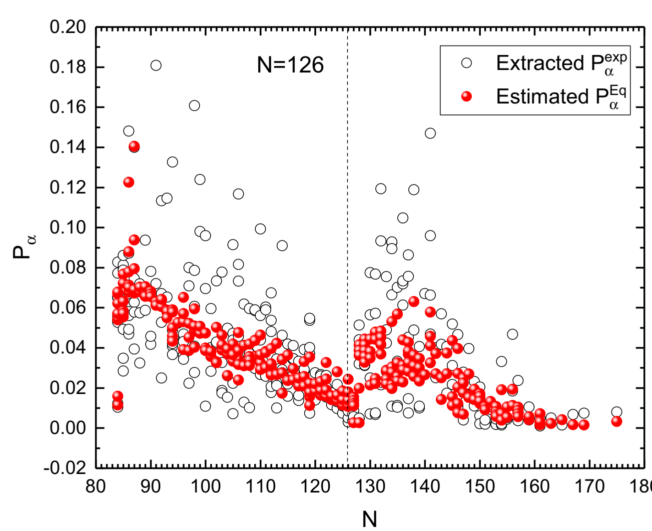

FIG. 2. Same as Fig. 1, but depicting the extracted experimental α-particle preformation factor P_α^{exp} from Eq. (20) and the estimated one P_α^{Eq} by Eq. (21) of odd-A nuclei.

TABLE IV. Same as Tables II and III, but for α decay of doubly odd nuclei.

α transition		Q_α	l_{min}	$\log_{10} T_{1/2}^{exp}$	$\log_{10} T_{1/2}^{cal1}$	P_α^{exp}	P_α^{Eq}	$\log_{10} T_{1/2}^{cal2}$
^{148}Eu	^{144}Pm	2.69	0	14.98	13.77	0.0614	0.0509	15.06
^{152}Ho	^{148}Tb	4.51	0	3.12	1.83	0.0511	0.0433	3.19
^{152}Ho^m	^{148}Tb^m	4.58	0	2.66	1.44	0.0595	0.0434	2.8
^{154}Ho	^{150}Tb	4.04	0	6.56	4.65	0.0123	0.0397	6.05
^{154}Tm	^{150}Ho	5.09	0	1.17	−0.16	0.0466	0.0405	1.23
^{154}Tm^m	^{150}Ho^m	5.18	0	0.75	−0.54	0.0506	0.0406	0.85
^{156}Tm	^{152}Ho	4.35	0	5.12	3.88	0.0586	0.0366	5.32
^{156}Lu^m	^{152}Tm^m	5.72	0	−0.68	−1.96	0.0526	0.0382	−0.54
^{158}Ta	^{154}Lu	6.13	0	−1.29	−2.71	0.0384	0.0359	−1.27
^{158}Ta^m	^{154}Lu^m	6.21	0	−1.42	−3.01	0.0257	0.036	−1.57
^{160}Re	^{156}Ta	6.7	2	−2.26	−3.6	0.0459	0.0203	−1.9
^{162}Re	^{158}Ta	6.25	0	−0.95	−2.32	0.0428	0.0311	−0.81
^{162}Re^m	^{158}Ta^m	6.28	0	−1.07	−2.43	0.0441	0.0311	−0.92
^{164}Re^m	^{160}Ta^m	5.77	0	1.46	−0.43	0.013	0.0282	1.12
^{164}Ir^m	^{160}Re^m	7.06	0	−2.78	−4.36	0.026	0.0299	−2.84
^{166}Ir	^{162}Re	6.73	0	−1.95	−3.29	0.0459	0.0275	−1.73
^{166}Ir^m	^{162}Re^m	6.73	0	−1.81	−3.29	0.0336	0.0275	−1.73
^{168}Ir	^{164}Re	6.38	0	−0.64	−2.04	0.0401	0.0251	−0.43
^{168}Ir^m	^{164}Re^m	6.48	0	−0.68	−2.41	0.0185	0.0253	−0.82
^{170}Ir	^{166}Re^p	5.96	0	1.24	−0.37	0.0245	0.0228	1.27
^{170}Ir^m	^{166}Re	6.27	2	0.35	−1.32	0.0214	0.014	0.54
^{172}Ir	^{168}Re	5.99	3	2.34	0.06	0.0052	0.0104	2.04
^{172}Ir^m	^{168}Re	6.13	0	1.36	−1.16	0.003	0.0217	0.51
^{174}Ir	^{170}Re	5.63	2	3.17	1.31	0.0137	0.0117	3.24
^{174}Ir^m	^{170}Re	5.82	2	2.29	0.44	0.0142	0.0119	2.37
^{170}Au	^{166}Ir	7.18	0	−2.58	−4.03	0.0361	0.0243	−2.41
^{170}Au^m	^{166}Ir^m	7.29	0	−2.84	−4.38	0.0283	0.0245	−2.77
^{176}Au	^{172}Ir	6.44	0	0.14	−1.52	0.0217	0.019	0.2
^{186}Au	^{182}Ir	4.91	1	7.89	5.59	0.005	0.0088	7.65
^{180}Tl	^{176}Au^m	6.57	3	1.23	−0.62	0.0141	0.0079	1.48
^{186}Tl^m	^{182}Au	6.02	6	5.66	3.01	0.0022	0.0033	5.49
^{186}Bi	^{182}Tl	7.76	1	−1.83	−4.51	0.0021	0.0108	−2.54
^{186}Bi^m	^{182}Tl^m	7.88	3	−2.01	−4.38	0.0042	0.0071	−2.23
^{190}Bi	^{186}Tl	6.86	1	0.91	−1.56	0.0033	0.0089	0.49
^{190}Bi^m	^{186}Tl^m	6.97	3	0.94	−1.45	0.0041	0.0058	0.79
^{192}Bi	^{188}Tl	6.38	1	2.44	0.29	0.0071	0.008	2.39
^{192}Bi^m	^{188}Tl^m	6.49	3	2.58	0.36	0.006	0.0052	2.65
^{194}Bi	^{190}Tl	5.92	1	4.31	2.25	0.0086	0.0071	4.4
^{194}Bi^n	^{190}Tl^m	6.02	3	4.74	2.31	0.0036	0.0047	4.63
^{196}Bi	^{192}Tl^p	5.26	0	7.42	5.46	0.0109	0.0083	7.54
^{196}Bi^n	^{192}Tl^n	5.32	2	7.8	5.45	0.0045	0.005	7.75
^{212}Bi	^{208}Tl	6.21	5	4	1.99	0.0097	0.0058	4.23
^{214}Bi	^{210}Tl	5.62	5	6.75	4.73	0.0094	0.0064	6.92
^{192}At	^{188}Bi	7.7	0	−1.94	−3.72	0.0164	0.0117	−1.79
^{192}At^m	^{188}Bi^m	7.63	3	−1.06	−2.94	0.0131	0.0056	−0.69
^{194}At	^{190}Bi^n	7.33	0	−0.54	−2.59	0.009	0.0107	−0.62
^{194}At^m	^{190}Bi^m	7.31	0	−0.49	−2.49	0.01	0.0107	−0.52
^{200}At	^{196}Bi	6.6	0	1.92	0.06	0.0141	0.0083	2.15
^{200}At^n	^{196}Bi^m	6.77	3	1.88	−0.05	0.0116	0.0041	2.33
^{202}At	^{198}Bi	6.35	0	3.16	0.99	0.0068	0.0076	3.11
^{202}At^m	^{198}Bi^m	6.26	0	3.32	1.4	0.012	0.0075	3.52
^{202}At^n	^{198}Bi^n	6.4	0	2.68	0.79	0.0128	0.0076	2.91
^{204}At	^{200}Bi	6.07	0	4.16	2.22	0.0115	0.0069	4.38
^{206}At	^{202}Bi	5.89	0	5.31	3.06	0.0057	0.0063	5.26
^{208}At	^{204}Bi	5.75	0	6.02	3.7	0.0048	0.0059	5.93
^{210}At	^{206}Bi	5.63	2	7.22	4.52	0.002	0.0032	7.02
^{212}At	^{208}Bi	7.82	5	−0.5	−3.1	0.0025	0.0041	−0.71
^{218}At	^{214}Bi	6.87	0	0.18	−1.38	0.0277	0.0334	0.09

TABLE IV. (*Continued.*)

α transition		Q_α	l_{min}	$\log_{10} T_{1/2}^{exp}$	$\log_{10} T_{1/2}^{cal1}$	P_α^{exp}	P_α^{Eq}	$\log_{10} T_{1/2}^{cal2}$
^{220}At	^{216}Bi^m	6.05	0	3.43	2.02	0.0382	0.0368	3.45
^{200}Fr^m	^{196}At^m	7.71	0	−0.72	−3.11	0.0041	0.0089	−1.06
^{212}Fr	^{208}At	6.53	2	3.44	1.27	0.0068	0.0033	3.76
^{214}Fr	^{210}At	8.59	5	−2.29	−4.66	0.0042	0.0039	−2.25
^{218}Fr	^{214}At	8.01	0	−3	−4.43	0.0369	0.0341	−2.97
^{218}Fr^m	^{214}At^n	7.87	2	−1.66	−3.7	0.009	0.0115	−1.76
^{220}Fr	^{216}At	6.8	1	1.44	−0.16	0.0253	0.0198	1.54
^{216}Ac	^{212}Fr	9.24	5	−3.36	−5.74	0.0042	0.0042	−3.36
^{216}Ac^m	^{212}Fr	9.28	5	−3.36	−5.84	0.0032	0.0041	−3.46
^{218}Ac	^{214}Fr	9.37	0	−6	−7.43	0.0372	0.0394	−6.02
^{222}Ac	^{218}Fr	7.14	0	0.7	−0.72	0.0378	0.0375	0.71
^{226}Ac	^{222}Fr	5.51	2	9.23	6.98	0.0056	0.0112	8.93
^{220}Pa	^{216}Ac	9.65	0	−6.11	−7.45	0.045	0.0468	−6.12
^{224}Pa	^{220}Ac	7.69	2	−0.07	−1.64	0.027	0.0119	0.28
^{228}Pa	^{224}Ac	6.27	3	6.63	4.25	0.0042	0.0056	6.51
^{230}Pa	^{226}Ac	5.44	2	10.67	8.27	0.004	0.008	10.37
^{242}Am^m	^{238}Np	5.64	3	11.99	9.26	0.0018	0.0013	12.15
^{246}Es	^{242}Bk^p	7.5	0	3.66	1.65	0.0099	0.0073	3.79
^{248}Es	^{244}Bk	7.16	2	5.76	3.24	0.003	0.0017	6.01
^{252}Es	^{248}Bk	6.79	2	7.72	4.83	0.0013	0.001	7.83
^{254}Es^m	^{250}Bk	6.7	1	7.64	4.96	0.0021	0.0012	7.88
^{256}Md^m	^{252}Es	7.91	3	4.7	1.27	0.0004	0.0006	4.49
^{258}Md	^{254}Es	7.27	1	6.65	3.29	0.0004	0.001	6.29

Eq. (20) with $\log_{10} T_{1/2}^{cal1}$ and $\log_{10} T_{1/2}^{exp}$. The eighth column is the estimated α-particle preformation factor by Eq. (21). The last column is the calculated α decay half-life within GLDM with the estimated α-particle preformation factor by Eq. (21). From these three tables, we can find that for most nuclei, when $P_\alpha = 1$, calculated α decay half-lives $\log_{10} T_{1/2}^{cal1}$ are smaller than experimental data by more than an order of magnitude, which shows that the α preformation factors $P_\alpha = 1$ are overestimated. Noticeably, one can find that after considering α-particle preformation factors P_α^{Eq} estimated by Eq. (21), $\log_{10} T_{1/2}^{cal2}$ can well reproduce experimental α decay half-lives in the region of 10^{-8} to 10^{26} s.

For the sake of clarity, the differences between the logarithmic values of two calculated α decay half-lives $\log_{10} T_{1/2}^{cal1}$ and $\log_{10} T_{1/2}^{cal2}$, and experimental data are denoted as solid blue stars and red circles, and are plotted

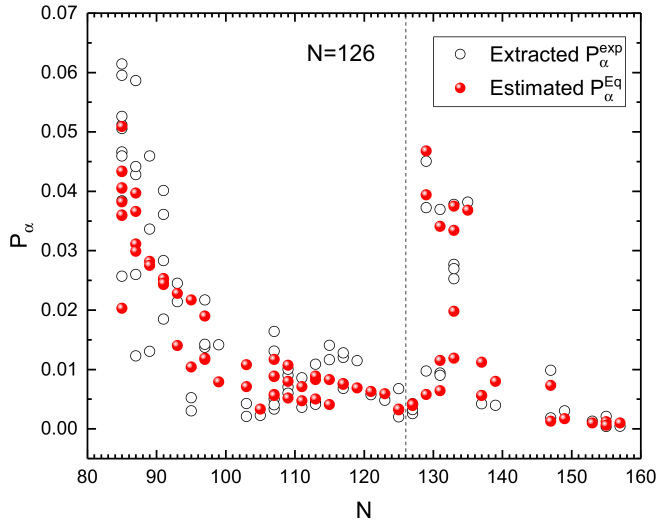

FIG. 3. Same as Fig. 1, but depicting the extracted experimental α-particle preformation factor P_α^{exp} from Eq. (20) and the estimated one P_α^{Eq} by Eq. (21) of doubly odd nuclei.

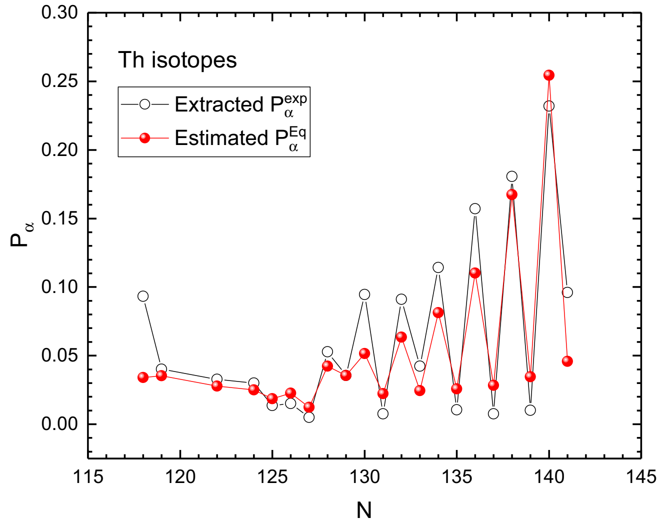

FIG. 4. Same as Fig. 1, but depicting the extracted experimental α-particle preformation factor P_α^{exp} from Eq. (20) and the estimated one P_α^{Eq} by Eq. (21) of Th isotopes.

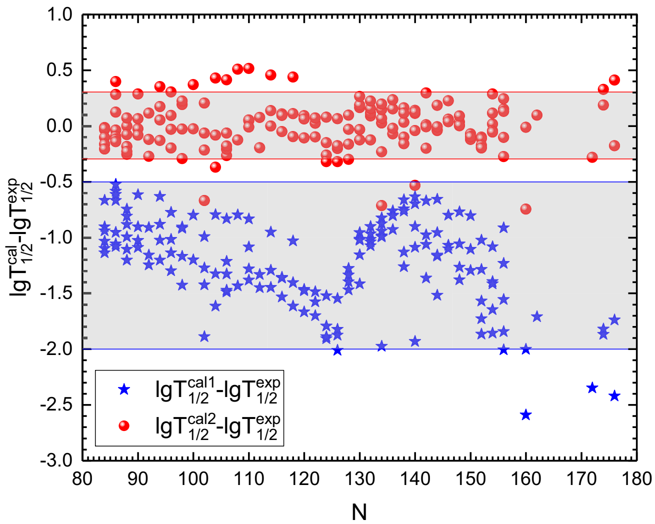

FIG. 5. The logarithmic differences between two calculated α decay half-lives and experimental data of even-even nuclei. The solid blue star and red circle denote the differences caused by $\log_{10} T^{\text{cal1}}_{1/2}$ and $\log_{10} T^{\text{cal2}}_{1/2}$.

in Figs. 5–7 for even-even nuclei, odd-A nuclei, and doubly odd nuclei, respectively. From these figures, we can find that $\log_{10} T^{\text{cal1}}_{1/2}$ are significantly lower than experimental data. In particular, $\log_{10} T^{\text{cal1}}_{1/2}$ are basically more than two orders of magnitude smaller than experimental data for superheavy nuclei. Noticeably, after considering α-particle preformation factors obtained by Eq. (21), the deviations caused by $\log_{10} T^{\text{cal2}}_{1/2}$ are around zero, showing that global $\log_{10} T^{\text{cal2}}_{1/2}$ can well reproduce experimental data and significantly reduce the deviations. This formula can be extended to estimate α-particle preformation factors and to predict α

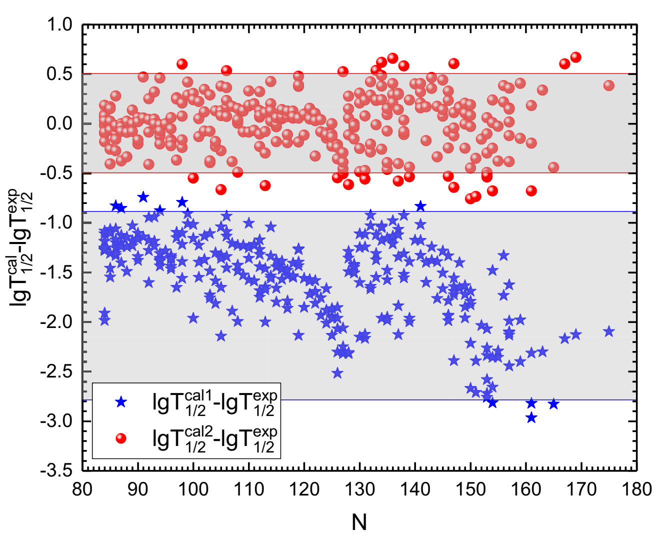

FIG. 6. Same as Fig. 5, but depicting the logarithmic differences between two calculated α decay half-lives and experimental data of odd-A nuclei.

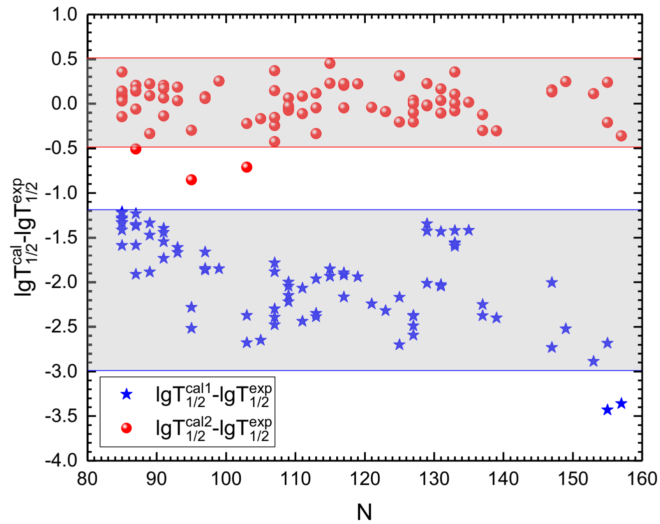

FIG. 7. Same as Fig. 5, but depicting the logarithmic differences between two calculated α decay half-lives and experimental data of doubly odd nuclei.

decay half-lives for unsynthesized superheavy nuclei, which would be useful for future experiments in synthesizing new superheavy elements and isotopes. For all 535 nuclei, the standard deviation between $\log_{10} T^{\text{cal2}}_{1/2}$ and $\log_{10} T^{\text{exp}}_{1/2}$ is $\sigma = 0.257$, indicating calculated α decay half-lives using GLDM with α-particle preformation factors obtained by our proposed formula can reproduce experimental data within a factor of $10^{0.257} = 1.81$.

IV. SUMMARY

In summary, a bridge between the α decay energy and α-particle preformation factor is built. An analytical expression for estimating the α-particle preformation factor is proposed. This formula can help to accurately calculate α decay half-lives, and can be extended to estimate α-particle preformation factors as well as predict the α decay half-lives for unsynthesized superheavy nuclei, which would be useful for future experiments in synthesizing new superheavy elements and isotopes. This formula can also shed light on some microscopic nuclear structure information, such as the shell effect and the odd-even staggering effect. It also provides a positive signal for the existence of an island of stability for superheavy nuclei.

ACKNOWLEDGMENTS

This work is supported by the National Natural Science Foundation of China (Grants No. 10775061, No. 11175054, No. 11675066, No. 11665019, and No. 11947229), by the Fundamental Research Funds for the Central Universities (Grants No. lzujbky-2017-ot04 and No. lzujbky-2020-it01), and by the Feitian Scholar Project of Gansu province.

[1] R. W. Gurney and E. U. Condon, Nature (London) **122**, 439 (1928).
[2] G. Gamow, Z. Phys. **51**, 204 (1928).
[3] D. Geesaman, C. Gelbke, R. Janssens, and B. Sherrill, Annu. Rev. Nucl. Part. Sci. **56**, 53 (2006).
[4] S. Hofmann and G. Münzenberg, Rev. Mod. Phys. **72**, 733 (2000).
[5] M. Pfützner, M. Karny, L. V. Grigorenko, and K. Riisager, Rev. Mod. Phys. **84**, 567 (2012).
[6] A. N. Andreyev, M. Huyse, P. Van Duppen, C. Qi, R. J. Liotta, S. Antalic, D. Ackermann, S. Franchoo, F. P. Heßberger, S. Hofmann, I. Kojouharov, B. Kindler, P. Kuusiniemi, S. R. Lesher, B. Lommel, R. Mann, K. Nishio, R. D. Page, B. Streicher, Š. Šáro, B. Sulignano, D. Wiseman, and R. A. Wyss, Phys. Rev. Lett. **110**, 242502 (2013).
[7] L. Ma, Z. Y. Zhang, Z. G. Gan, H. B. Yang, L. Yu, J. Jiang, J. G. Wang, Y. L. Tian, Y. S. Wang, S. Guo, B. Ding, Z. Z. Ren, S. G. Zhou, X. H. Zhou, H. S. Xu, and G. Q. Xiao, Phys. Rev. C **91**, 051302(R) (2015).
[8] W. M. Seif, Phys. Rev. C **74**, 034302 (2006).
[9] J. Khuyagbaatar, A. Yakushev, C. E. Düllmann, D. Ackermann, L.-L. Andersson, M. Asai, M. Block, R. A. Boll, H. Brand, D. M. Cox, M. Dasgupta, X. Derkx, A. Di Nitto, K. Eberhardt, J. Even, M. Evers, C. Fahlander, U. Forsberg, J. M. Gates, N. Gharibyan *et al.*, Phys. Rev. Lett. **112**, 172501 (2014).
[10] R. J. Carroll, R. D. Page, D. T. Joss, J. Uusitalo, I. G. Darby, K. Andgren, B. Cederwall, S. Eeckhaudt, T. Grahn, C. Gray-Jones, P. T. Greenlees, B. Hadinia, P. M. Jones, R. Julin, S. Juutinen, M. Leino, A.-P. Leppänen, M. Nyman, D. O'Donnell, J. Pakarinen, P. Rahkila, M. Sandzelius, J. Sarén, C. Scholey, D. Seweryniak, and J. Simpson, Phys. Rev. Lett. **112**, 092501 (2014).
[11] D. S. Delion, R. J. Liotta, and R. Wyss, Phys. Rev. C **92**, 051301(R) (2015).
[12] W. M. Seif, M. Shalaby, and M. F. Alrakshy, Phys. Rev. C **84**, 064608 (2011).
[13] Y. Ren and Z. Ren, Phys. Rev. C **85**, 044608 (2012).
[14] Y. Qian, Z. Ren, and D. Ni, Phys. Rev. C **89**, 024318 (2014).
[15] Z. Ren, Phys. Rev. C **65**, 051304(R) (2002).
[16] D. Ni and Z. Ren, Ann. Phys. (NY) **358**, 108 (2015).
[17] M. Brack, J. Damgaard, A. S. Jensen, H. C. Pauli, V. M. Strutinsky, and C. Y. Wong, Rev. Mod. Phys. **44**, 320 (1972).
[18] D. N. Poenaru, I. H. Plonski, R. A. Gherghescu, and W. Greiner, J. Phys. G **32**, 1223 (2006).
[19] A. Parkhomenko and A. Sobiczewski, Acta Phys. Pol. B **36**, 1363 (2005).
[20] Y. T. Oganessian, V. K. Utyonkov, Y. V. Lobanov, F. S. Abdullin, A. N. Polyakov, R. N. Sagaidak, I. V. Shirokovsky, Y. S. Tsyganov, A. A. Voinov, G. G. Gulbekian, S. L. Bogomolov, B. N. Gikal, A. N. Mezentsev, V. G. Subbotin, A. M. Sukhov, K. Subotic, V. I. Zagrebaev, G. K. Vostokin, M. G. Itkis, R. A. Henderson, J. M. Kenneally, J. H. Landrum, K. J. Moody, D. A. Shaughnessy, M. A. Stoyer, N. J. Stoyer, and P. A. Wilk, Phys. Rev. C **76**, 011601(R) (2007).
[21] P. A. Ellison, K. E. Gregorich, J. S. Berryman, D. L. Bleuel, R. M. Clark, I. Dragojević, J. Dvorak, P. Fallon, C. Fineman-Sotomayor, J. M. Gates, O. R. Gothe, I. Y. Lee, W. D. Loveland, J. P. McLaughlin, S. Paschalis, M. Petri, J. Qian, L. Stavsetra, M. Wiedeking, and H. Nitsche, Phys. Rev. Lett. **105**, 182701 (2010).
[22] Y. T. Oganessian, F. S. Abdullin, P. D. Bailey, D. E. Benker, M. E. Bennett, S. N. Dmitriev, J. G. Ezold, J. H. Hamilton, R. A. Henderson, M. G. Itkis, Y. V. Lobanov, A. N. Mezentsev, K. J. Moody, S. L. Nelson, A. N. Polyakov, C. E. Porter, A. V. Ramayya, F. D. Riley, J. B. Roberto, M. A. Ryabinin, K. P. Rykaczewski, R. N. Sagaidak, D. A. Shaughnessy, I. V. Shirokovsky, M. A. Stoyer, V. G. Subbotin, R. Sudowe, A. M. Sukhov, Y. S. Tsyganov, V. K. Utyonkov, A. A. Voinov, G. K. Vostokin, and P. A. Wilk, Phys. Rev. Lett. **104**, 142502 (2010).
[23] J. H. Hamilton., S. Hofmann, and Y. T. Oganessian, Ann. Rev. Nucl. Part. Sci. **63**, 383 (2013).
[24] K. Morita, K. Morimoto, D. Kaji, T. Akiyama, S. ichi Goto, H. Haba, E. Ideguchi, K. Katori, H. Koura, H. Kikunaga, H. Kudo, T. Ohnishi, A. Ozawa, N. Sato, T. Suda, K. Sueki, F. Tokanai, T. Yamaguchi, A. Yoneda, and A. Yoshida, J. Phys. Soc. Jpn. **76**, 045001 (2007).
[25] Y. T. Oganessian, Radiochim. Acta **99**, 429 (2011).
[26] J.-G. Deng, X.-H. Li, J.-L. Chen, J.-H. Cheng, and X.-J. Wu, Eur. Phys. J. A **55**, 58 (2019).
[27] B. Buck, A. C. Merchant, and S. M. Perez, J. Phys. G **17**, L91 (1991).
[28] J.-G. Deng, J.-C. Zhao, P.-C. Chu, and X.-H. Li, Phys. Rev. C **97**, 044322 (2018).
[29] J.-G. Deng, J.-C. Zhao, D. Xiang, and X.-H. Li, Phys. Rev. C **96**, 024318 (2017).
[30] D. S. Delion, Phys. Rev. C **80**, 024310 (2009).
[31] D. N. Poenaru, R. A. Gherghescu, and W. Greiner, Phys. Rev. C **83**, 014601 (2011).
[32] J. M. Dong, H. F. Zhang, and G. Royer, Phys. Rev. C **79**, 054330 (2009).
[33] K. Santhosh, S. Sahadevan, B. Priyanka, and M. Unnikrishnan, Nucl. Phys. A **882**, 49 (2012).
[34] X. J. Bao, S. Q. Guo, H. F. Zhang, Y. Z. Xing, J. M. Dong, and J. Q. Li, J. Phys. G **42**, 085101 (2015).
[35] D. N. Poenaru, H. Stöcker, and R. A. Gherghescu, Eur. Phys. J. A **54**, 14 (2018).
[36] D. N. Poenaru and W. Greiner, Phys. Scr. **44**, 427 (1991).
[37] D. N. Poenaru, R. A. Gherghescu, and W. Greiner, J. Phys. G **40**, 105105 (2013).
[38] D. N. Poenaru and R. A. Gherghescu, Phys. Rev. C **94**, 014309 (2016).
[39] H. F. Zhang and G. Royer, Phys. Rev. C **77**, 054318 (2008).
[40] R. G. Lovas, R. J. Liotta, A. Insolia, K. Varga, and D. S. Delion, Phys. Rep. **294**, 265 (1998).
[41] K. Varga, R. G. Lovas, and R. J. Liotta, Phys. Rev. Lett. **69**, 37 (1992).
[42] I. Tonozuka and A. Arima, Nucl. Phys. A **323**, 45 (1979).
[43] G. Dodig-Crnkovic, F. Janouch, and R. Liotta, Nucl. Phys. A **501**, 533 (1989).
[44] K. Varga, R. Lovas, and R. Liotta, Nucl. Phys. A **550**, 421 (1992).
[45] G. Röpke, P. Schuck, Y. Funaki, H. Horiuchi, Z. Ren, A. Tohsaki, C. Xu, T. Yamada, and B. Zhou, Phys. Rev. C **90**, 034304 (2014).
[46] C. Xu, Z. Ren, G. Röpke, P. Schuck, Y. Funaki, H. Horiuchi, A. Tohsaki, T. Yamada, and B. Zhou, Phys. Rev. C **93**, 011306(R) (2016).
[47] H. F. Zhang, G. Royer, and J. Q. Li, Phys. Rev. C **84**, 027303 (2011).
[48] Y. Qian and Z. Ren, Sci. China Phys., Mech. Astron. **56**, 1520 (2013).

[49] G. L. Zhang, X. Y. Le, and H. Q. Zhang, Phys. Rev. C **80**, 064325 (2009).
[50] J.-G. Deng, J.-H. Cheng, B. Zheng, and X.-H. Li, Chin. Phys. C **41**, 124109 (2017).
[51] J.-G. Deng, J.-C. Zhao, J.-L. Chen, X.-J. Wu, and X.-H. Li, Chin. Phys. C **42**, 044102 (2018).
[52] S. M. S. Ahmed, R. Yahaya, S. Radiman, and M. S. Yasir, J. Phys. G **40**, 065105 (2013).
[53] D. Deng, Z. Ren, D. Ni, and Y. Qian, J. Phys. G **42**, 075106 (2015).
[54] D. Deng and Z. Ren, Phys. Rev. C **93**, 044326 (2016).
[55] S. M. S. Ahmed, Nucl. Phys. A **962**, 103 (2017).
[56] G. Royer, J. Phys. G **26**, 1149 (2000).
[57] G. Royer, Nucl. Phys. A **848**, 279 (2010).
[58] J.-G. Deng, H.-F. Zhang, and G. Royer, Phys. Rev. C **101**, 034307 (2020).
[59] C. Qi, F. R. Xu, R. J. Liotta, and R. Wyss, Phys. Rev. Lett. **103**, 072501 (2009).
[60] V. Y. Denisov and A. A. Khudenko, Phys. Rev. C **79**, 054614 (2009).
[61] Z. Y. Wang, Z. M. Niu, Q. Liu, and J. Y. Guo, J. Phys. G **42**, 055112 (2015).
[62] H. C. Manjunatha and K. N. Sridhar, Eur. Phys. J. A **53**, 156 (2017).
[63] D. T. Akrawy, H. Hassanabadi, S. Hosseini, and K. Santhosh, Nucl. Phys. A **971**, 130 (2018).
[64] G. Royer and H. F. Zhang, Phys. Rev. C **77**, 037602 (2008).
[65] D. T. Akrawy and D. N. Poenaru, J. Phys. G **44**, 105105 (2017).
[66] K. Santhosh and C. Nithya, At. Data Nucl. Data Tables **119**, 33 (2018).
[67] K. Santhosh and C. Nithya, At. Data Nucl. Data Tables **121–122**, 216 (2018).
[68] Y. Z. Wang, S. J. Wang, Z. Y. Hou, and J. Z. Gu, Phys. Rev. C **92**, 064301 (2015).
[69] C. Qi, R. Liotta, and R. Wyss, Prog. Part. Nucl. Phys. **105**, 214 (2019).
[70] H. Zhang, W. Zuo, J. Li, and G. Royer, Phys. Rev. C **74**, 017304 (2006).
[71] H. F. Zhang and G. Royer, Phys. Rev. C **76**, 047304 (2007).
[72] Y. Z. Wang, H. F. Zhang, J. M. Dong, and G. Royer, Phys. Rev. C **79**, 014316 (2009).
[73] X. Bao, H. Zhang, H. Zhang, G. Royer, and J. Li, Nucl. Phys. A **921**, 85 (2014).
[74] G. Royer and B. Remaud, Nucl. Phys. A **444**, 477 (1985).
[75] X. J. Bao, H. F. Zhang, B. S. Hu, G. Royer, and J. Q. Li, J. Phys. G **39**, 095103 (2012).
[76] G. Royer and K. Zbiri, Nucl. Phys. A **697**, 630 (2002).
[77] B. Buck, A. C. Merchant, and S. M. Perez, Phys. Rev. C **45**, 2247 (1992).
[78] B. Buck, A. Merchant, and S. Perez, At. Data Nucl. Data Tables **54**, 53 (1993).
[79] C. Xu and Z. Ren, Phys. Rev. C **73**, 041301(R) (2006).
[80] C. Xu and Z. Ren, Phys. Rev. C **74**, 014304 (2006).
[81] D. Ni and Z. Ren, Phys. Rev. C **81**, 024315 (2010).
[82] Y. Qian, Z. Ren, and D. Ni, Phys. Rev. C **83**, 044317 (2011).
[83] G. Audi, F. Kondev, M. Wang, W. Huang, and S. Naimi, Chin. Phys. C **41**, 030001 (2017).
[84] W. Huang, G. Audi, M. Wang, F. Kondev, S. Naimi, and X. Xu, Chin. Phys. C **41**, 030002 (2017).
[85] M. Wang, G. Audi, F. Kondev, W. Huang, S. Naimi, and X. Xu, Chin. Phys. C **41**, 030003 (2017).